

Approximation properties relative to continuous scale space for hybrid discretisations of Gaussian derivative operators

Tony Lindeberg

Received: date / Accepted: date

Abstract This paper presents an analysis of properties of two hybrid discretisation methods for Gaussian derivatives, based on convolutions with either the normalised sampled Gaussian kernel or the integrated Gaussian kernel followed by central differences. The motivation for studying these discretisation methods is that in situations when multiple spatial derivatives of different orders are needed at the same scale level, they can be computed significantly more efficiently, compared to more direct derivative approximations based on explicit convolutions with either sampled Gaussian derivative kernels or integrated Gaussian derivative kernels.

We characterise the properties of these hybrid discretisation methods in terms of quantitative performance measures, concerning the amount of spatial smoothing that they imply, as well as the relative consistency of scale estimates obtained from scale-invariant feature detectors with automatic scale selection, with an emphasis on the behaviour for very small values of the scale parameter, which may differ significantly from corresponding results obtained from the fully continuous scale-space theory, as well as between different types of discretisation methods.

The presented results are intended as a guide, when designing as well as interpreting the experimental results of scale-space algorithms that operate at very fine scale levels.

Keywords scale · discrete · continuous · Gaussian kernel · Gaussian derivative · scale space

The support from the Swedish Research Council (contract 2022-02969) is gratefully acknowledged.

Tony Lindeberg
Computational Brain Science Lab, Division of Computational Science and Technology, KTH Royal Institute of Technology, SE-100 44 Stockholm, Sweden. E-mail: tony@kth.se, ORCID: 0000-0002-9081-2170.

1 Introduction

When analysing image data by automated methods, a fundamental constraint originates from the fact that natural images may contain different types of structures at different spatial scales. For this reason, the notion of scale-space representation (Iijima 1962; Witkin 1983; Koenderink 1984; Koenderink and van Doorn 1987, 1992; Lindeberg 1993a, 1994, 2011; Florack 1997; Weickert *et al.* 1999; ter Haar Romeny 2003) has been developed to process the image data at multiple scales, in such a way that different types of image features can be obtained depending on the spatial extent of the image operators. Specifically, according to both theoretical and empirical findings in the area of scale-space theory, Gaussian derivative responses, or approximations thereof, can be used as a powerful basis for expressing a rich variety of feature detectors, in terms of provably scale-covariant or scale-invariant image operations, that can in an automated manner handle variabilities in scale, caused by varying the distance between the observed objects and the camera (Lindeberg 1998a, 1998a, 2013b, 2013a, 2015, 2021a; Bretzner and Lindeberg 1998; Chomat *et al.* 2000; Lowe 2004; Bay *et al.* 2008). More recently, Gaussian derivative operators have also been used as a basis, to formulate parameterised mathematical primitives, to be used as the layers in deep networks (Jacobsen *et al.* 2016; Worrall and Welling 2019; Lindeberg 2020, 2022; Pintea *et al.* 2021; Sangalli *et al.* 2022; Penaud-Polge *et al.* 2022; Yang *et al.* 2023; Gavilima-Pilataxi and Ibarra-Fiallo 2023).

When to implement the underlying Gaussian derivative operators in scale-space theory in practice, special attention does, however, need to be taken concerning the fact that most of the scale-space formulations are based on continuous signals or images (see Appendix A for a conceptual background), while real-world signals and images are discrete (Lindeberg 1990, 1993a, 2024). Thus, when discretis-

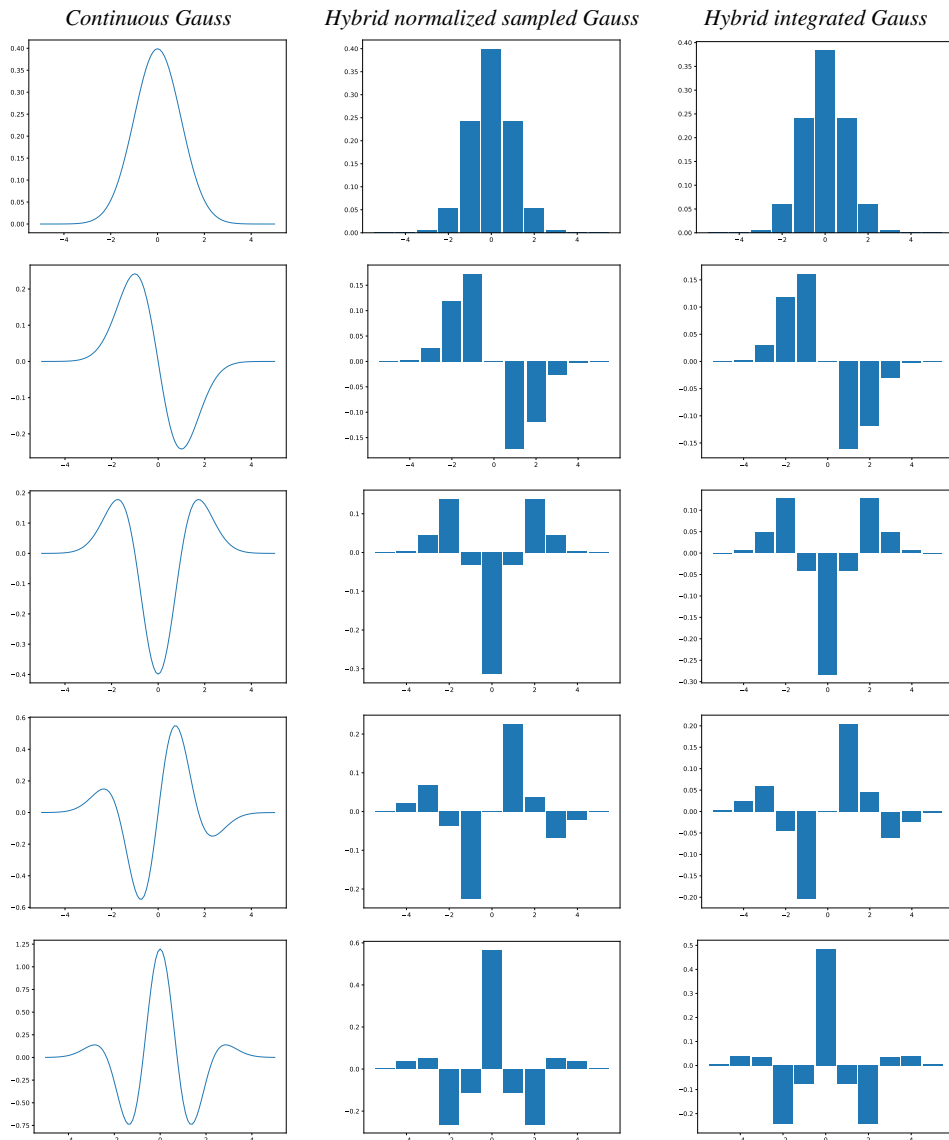


Fig. 1: Graphs of the main types of Gaussian smoothing kernels as well as of the equivalent convolution kernels for the hybrid discretisations of Gaussian derivative operators considered specially in this paper, here at the scale $\sigma = 1$, with the raw smoothing kernels in the top row and the order of spatial differentiation increasing downwards up to order 4: **(left column)** continuous Gaussian kernel and continuous Gaussian derivatives, **(middle column)** normalised sampled Gaussian kernel and central differences applied to the normalised sampled Gaussian kernel, **(right column)** integrated Gaussian kernel and central differences applied to the integrated Gaussian kernel. Note that the scaling of the vertical axis may vary between the different subfigures. **(Horizontal axes:** the 1-D spatial coordinate $x \in [-5, 5]$.) (Graphs of the regular sampled Gaussian derivative kernels, the regular integrated Gaussian derivative kernels and the discrete analogues of Gaussian derivatives up to order 4 are shown in Figure 1 in (Lindeberg 2024).)

ing the composed effect of the underlying Gaussian smoothing operation and the following derivative computations, it is essential to ensure that the desirable properties of the theoretically well-founded scale-space representations are to a sufficiently good degree of approximation transferred to the discrete implementation. Simultaneously, the amount of necessary computations needed for the implementation may often constitute a limiting factor, when to choose an appro-

priate discretisation method for expressing the actual algorithms, that are to operate on the discrete data to be analysed.

While one may argue that at sufficiently coarse scale levels, it ought to be the case that the choice of discretisation method should not significantly affect the quality of the output of a scale-space algorithm, at very fine scale levels, on the other hand, the properties of a discretised implementation of notions from scale-space theory may depend strongly on the actual choice of a discretisation method.

The subject of this article, is to perform a more detailed analysis of a class of hybrid discretisation methods, based on convolution with either the normalised sampled Gaussian kernel or the integrated Gaussian kernel, followed by computations of discrete derivative approximations by central difference operators, and specifically characterise the degree of approximation of continuous expressions in scale-space theory, that these discretisation give rise to, see Figure 1 for examples of graphs of equivalent convolution kernels corresponding to these discretisation methods. This class of discretisation methods was outlined among extensions to future work in Section 6.1 in (Lindeberg 2024), and was also complemented with a description about their theoretical properties in Footnote 13 in (Lindeberg 2024). There were, however, no further in-depth characterisations of the approximation properties of these discretisations, with regard to what results they lead to in relation to corresponding results from the continuous scale-space theory.

The main goal of this paper is to address this topic in terms of a set of quantitative performance measures, intended to be of general applicability for different types of visual tasks. Specifically, we will perform comparisons to the other main types of discretisation methods considered in (Lindeberg 2024), based on either (i) explicit convolutions with sampled Gaussian derivative kernels, (ii) explicit convolutions with integrated Gaussian derivative kernels, or (iii) convolution with the discrete analogue of the Gaussian kernel, followed by computations of discrete derivative approximations by central difference operators.

A main rationale for studying this class of hybrid discretisations is that in situations when multiple Gaussian derivative responses of different orders are needed at the same scale level, these hybrid discretisations imply substantially lower amounts of computations, compared to explicit convolutions with either sampled Gaussian derivative kernels or integrated Gaussian derivative kernels for each order of differentiation. The reason for this better computational efficiency, which also holds for the discretisation approach based on convolution with the discrete analogue of the Gaussian kernel followed by central differences, is that the spatial smoothing part of the operation, which is performed over a substantially larger number of input data than the small-support central difference operators, can be shared between the different orders of differentiation.

A further rationale for studying these hybrid discretisations is that in certain applications, such as the use of Gaussian derivative operators in deep learning architectures (Jacobsen *et al.* 2016, Lindeberg 2021c, 2022, Pintea *et al.* 2021, Sangalli *et al.* 2022, Penaud-Polge *et al.* 2022, Gavilima-Pilataxi and Ibarra-Fiallo 2023), the modified Bessel functions of integer order, as used as the underlying mathematical primitives in the discrete analogue of the Gaussian kernel, may, however, not be fully available in the framework

used for implementing the image processing operations. For this reason, the hybrid discretisations may, for efficiency reasons, constitute an interesting alternative to using discretisations in terms of either sampled Gaussian derivative kernels or integrated Gaussian derivative kernels, when to implement certain tasks, such as learning of the scale levels by backpropagation, which usually require full availability of the underlying mathematical primitives in the scale-parameterised filter family with regard to the deep learning framework, to be able to propagate the gradients between the layers in the deep learning architecture.

Deliberately, the scope of this paper is therefore to complement the in-depth treatment of discretisations of the Gaussian smoothing operation and the Gaussian derivative operators, and as a specific complement to the outline of the hybrid discretisations in the future work in (Lindeberg 2024).

We will therefore not consider other theoretically well-founded discretisations of scale-space operations (Wang 1999, Lim and Stiehl 2003, Tschirsich and Kuijper 2015, Slavík and Stehlík 2015, Rey-Otero and Delbraccio 2016). Nor will we consider alternative approaches in terms of pyramid representations (Burt and Adelson 1983, Crowley and Stern 1984, Simoncelli *et al.* 1992, Simoncelli and Freeman 1995, Lindeberg and Bretzner 2003, Crowley and Riff 2003, Lowe 2004), Fourier-based implementations, splines (Unser *et al.* 1991, 1993, Wang and Lee 1998, Bouma *et al.* 2007, Bekkers 2020, Zheng *et al.* 2022), recursive filters (Deriche 1992, Young and van Vliet 1995, van Vliet *et al.* 1998, Geusebroek *et al.* 2003, Farneböck and Westin 2006, Charalampidis 2016), or specific wavelet theory (Mallat 1989b, 1989a, 1999, 2016, Daubechies 1992, Meyer 1992, Teolis 1998, Debnath and Shah 2002).

Instead, we will focus on a selection of five specific methods, for implementing Gaussian derivative operations in terms of purely discrete convolution operations, and then with the emphasis on the behaviour for very small values of the scale parameter. This focus on very fine scale levels is particularly motivated from requirements regarding deep learning, where deep learning architectures often prefer to base their decisions on very fine-scale information, and specifically below the rule of thumb in classical computer vision, of not going trying to go to scale levels below a standard deviation $\sigma = \sqrt{s}$ of the Gaussian derivative kernels below, say $1/\sqrt{2}$ or 1, in units of the grid spacing.

2 Methods

The notion of scale-space representation is very general, and applies to wide classes of signals. Based on the separability property when computing Gaussian derivative responses in arbitrary dimensions (see Appendices B.1–B.2), we will in this section focus on discretisations of 1-D Gaussian derivative kernels. By separable extension over multiple dimen-

sions, this methodology can then be applied to signals, images and video over arbitrary numbers of dimensions.

2.1 Discretisation methods for 1-D Gaussian derivative operators

Given the definition of a scale-space representation of a one-dimensional continuous signal (Iijima 1962; Witkin 1983; Koenderink 1984; Koenderink and van Doorn 1987, 1992; Lindeberg 1993a, 1994, 2011; Florack 1997; Sporring *et al.* 1997; Weickert *et al.* 1999; ter Haar Romeny 2003), the 1-D Gaussian kernel is defined according to (for $x \in \mathbb{R}$):

$$g(x; s) = \frac{1}{\sqrt{2\pi s}} e^{-x^2/2s}, \quad (1)$$

where the parameter $s \in \mathbb{R}_+$ is referred to as the scale parameter, and any 1-D Gaussian derivative kernel for spatial differentiation order α is defined according to

$$g_{x^\alpha}(x; s) = \partial_{x^\alpha} g(x; s), \quad (2)$$

with the associated computation of Gaussian derivative responses from any 1-D input signal $f(x)$, in turn, defined according to

$$L_{x^\alpha}(x; s) = \int_{u \in \mathbb{R}} g_{x^\alpha}(u; s) f(x - u) du. \quad (3)$$

Let us first consider the following ways of approximating the Gaussian convolution operation for discrete data, based on convolutions with either (for $n \in \mathbb{Z}$):

- the sampled Gaussian kernel defined according to (see also Appendix B.3)

$$T_{\text{sampl}}(n; s) = g(n; s), \quad (4)$$

- the normalised sampled Gaussian kernel defined according to (see also Appendix B.4)

$$T_{\text{normsampl}}(n; s) = \frac{g(n; s)}{\sum_{m \in \mathbb{Z}} g(m; s)}, \quad (5)$$

- the integrated Gaussian kernel defined according to (Lindeberg 1993a Equation (3.89)) (see also Appendix B.5)

$$T_{\text{int}}(n; s) = \int_{x=n-1/2}^{n+1/2} g(x; s) dx, \quad (6)$$

- or the discrete analogue of the Gaussian kernel defined according to (Lindeberg 1990 Equation (19)) (see also Appendix B.6)

$$T_{\text{disc}}(n; s) = e^{-s} I_n(s), \quad (7)$$

where $I_n(s)$ denotes the modified Bessel functions of integer order (Abramowitz and Stegun 1964).

Then, we consider the following previously studied methods for discretising the computation of Gaussian derivative operators, in terms of either:

- convolutions with sampled Gaussian derivative kernels according to (see also Appendix B.7)

$$T_{\text{sampl}, x^\alpha}(n; s) = g_{x^\alpha}(n; s), \quad (8)$$

- convolutions with integrated Gaussian derivative kernels according to (Lindeberg 2024 Equation (54)) (see also Appendix B.8)

$$T_{\text{int}, x^\alpha}(n; s) = \int_{x=n-1/2}^{n+1/2} g_{x^\alpha}(x; s) dx, \quad (9)$$

- the genuinely discrete approach corresponding to convolution with the discrete analogue of the Gaussian kernel $T_{\text{disc}}(n; s)$ according to (7) followed by central difference operators δ_{x^α} , thus corresponding to the equivalent discrete approximation kernel (Lindeberg 1993b Equation (58)) (see also Appendix B.9)

$$T_{\text{disc}, x^\alpha}(n; s) = (\delta_{x^\alpha} T_{\text{disc}})(n; s). \quad (10)$$

Here, the central difference operators are for orders 1 and 2 defined according to

$$\delta_x = (-\frac{1}{2}, 0, +\frac{1}{2}), \quad (11)$$

$$\delta_{xx} = (+1, -2, +1), \quad (12)$$

and for higher values of α according to:

$$\delta_{x^\alpha} = \begin{cases} \delta_x (\delta_{xx})^i & \text{if } \alpha = 1 + 2i, \\ (\delta_{xx})^i & \text{if } \alpha = 2i, \end{cases} \quad (13)$$

for integer i , where the special cases $\alpha = 3$ and $\alpha = 4$ then correspond to the difference operators

$$\delta_{xxx} = (-\frac{1}{2}, +1, 0, -1, +\frac{1}{2}), \quad (14)$$

$$\delta_{xxxx} = (+1, -4, +6, -4, +1). \quad (15)$$

In addition to the above, already studied discretisation methods in (Lindeberg 2024), we will here specifically consider the properties of the following hybrid methods, in terms of either:

- the hybrid approach corresponding to convolution with the normalised sampled Gaussian kernel $T_{\text{normsampl}}(n; s)$ according to (5) followed by central difference operators δ_{x^α} according to (13), thus corresponding to the equivalent discrete approximation kernel (Lindeberg 2024 Equation (116)) (see also Appendix B.10)

$$T_{\text{hybr-sampl}, x^\alpha}(n; s) = (\delta_{x^\alpha} T_{\text{normsampl}})(n; s), \quad (16)$$

- the hybrid approach corresponding to convolution with the integrated Gaussian kernel $T_{\text{int}}(n; s)$ according to (6) followed by central difference operators δ_{x^α} according to (13), thus corresponding to the equivalent discrete approximation kernel (Lindeberg 2024 Equation (117)) (see also Appendix B.11)

$$T_{\text{hybr-int},x^\alpha}(n; s) = (\delta_{x^\alpha} T_{\text{int}})(n; s). \quad (17)$$

A motivation for introducing these hybrid discretisation methods (16) and (17), based on convolutions with the normalised sampled Gaussian kernel (5) or the integrated Gaussian kernel (6) followed by central difference operators of the form (13), is that these discretisation methods have substantially better computational efficiency, compared to explicit convolutions with either the sampled Gaussian derivative kernels (8) or the integrated Gaussian derivative kernels (9), in situations when spatial derivatives of multiple orders α are needed at the same scale level.

The reason for this is that the same spatial smoothing stage can then be shared between the computations of discrete derivative approximations for the different orders of spatial differentiation, thus implying that these hybrid methods will be as computationally efficient as the genuinely discrete approach, based on convolution with the discrete analogue of the Gaussian kernel (7) followed by central differences of the form (13), and corresponding to equivalent convolution kernels of the form (10).

2.1.1 Quantitative measures of approximation properties relative to continuous scale space

To measure how well the above discretisation methods for the Gaussian derivative operators reflect properties of the underlying continuous Gaussian derivatives, we will consider quantifications in terms of the following spatial spread measure, defined from spatial variance V of the absolute value of each equivalent discrete derivative approximation kernel (Lindeberg 2024 Equation (80)):

$$\sqrt{V(|T_{x^\alpha}(\cdot; s)|)}, \quad (18)$$

where the variance $V(h(\cdot))$ of a non-negative continuous 1-D function $h(x)$ is defined as

$$V(h(\cdot)) = \frac{\int_{x \in \mathbb{R}} x^2 h(x) dx}{\int_{x \in \mathbb{R}} h(x) dx} - \left(\frac{\int_{x \in \mathbb{R}} x h(x) dx}{\int_{x \in \mathbb{R}} h(x) dx} \right)^2. \quad (19)$$

To furthermore more explicitly quantify the deviation from the corresponding fully continuous spatial spread measures $\sqrt{V(|g_{x^\alpha}(\cdot; s)|)}$, we also consider the following measures of the offsets of the spatial spread measures (Lindeberg 2024 Equation (81)):

$$O_\alpha(s) = \sqrt{V(|T_{x^\alpha}(\cdot; s)|)} - \sqrt{V(|g_{x^\alpha}(\cdot; s)|)}, \quad (20)$$

where the variance $V(h(\cdot))$ of a non-negative discrete function $h(n)$ is defined as

$$V(h(\cdot)) = \frac{\sum_{n \in \mathbb{Z}} n^2 h(n)}{\sum_{n \in \mathbb{Z}} h(n)} - \left(\frac{\sum_{n \in \mathbb{Z}} n h(n)}{\sum_{n \in \mathbb{Z}} h(n)} \right)^2. \quad (21)$$

2.2 Methodology for characterising the resulting consistency properties over scale in terms of the accuracy of the scale estimates obtained from integrations with scale selection algorithms

To perform a further evaluation of the hybrid discretisation method to consistently process input data over multiple scales, we will characterise the abilities of these methods in a context of feature detection with automatic scale selection (Lindeberg 1998a, 1998a, 2021a), where hypotheses about local appropriate scale levels are determined from local extrema over scale of scale-normalised derivative responses.

For this purpose, we follow a similar methodology as used in (Lindeberg 2024 Section 4). Thus, with the theory in Section 2.1 now applied to 2-D image data, by separable application of the 1-D theory along each image dimension, we consider scale-normalised derivative operators defined according to (Lindeberg 1998a, 1998b) (for $(x, y) \in \mathbb{R}^2$ and $s \in \mathbb{R}_+$):

$$\partial_\xi = s^{\gamma/2} \partial_x, \quad \partial_\eta = s^{\gamma/2} \partial_y, \quad (22)$$

with $\gamma > 0$ being a scale normalisation power, that is chosen specially adapted for each feature detection task.

2.2.1 Scale-invariant feature detectors with automatic scale selection

Specifically, we will evaluate the performance of the following types of scale-invariant feature detectors, defined from the spatial derivatives $L_x(x, y; s)$, $L_y(x, y; s)$, $L_{xx}(x, y; s)$, $L_{xy}(x, y; s)$ and $L_{yy}(x, y; s)$ up to order 2 of the 2-D scale-space representation $L(x, y; s)$ of any 2-D image $f(x, y)$ at scale s , obtained by convolution with 2-D Gaussian kernels $g_{2D}(x, y; s)$ for different values of s :

- *interest point detection* from scale-space extrema (extrema over both space (x, y) and scale s) of the scale-normalised Laplacian operator (Lindeberg 1998a Equation (30))

$$\nabla_{\text{norm}}^2 L = s (L_{xx} + L_{yy}), \quad (23)$$

or the scale-normalised determinant of the Hessian operator (Lindeberg 1998a Equation (31))

$$\det \mathcal{H}_{\text{norm}} L = s^2 (L_{xx} L_{yy} - L_{xy}^2), \quad (24)$$

where we here choose the scale normalisation parameter $\gamma = 1$, such that the selected scale level for a Gaussian blob of size $s_0 \in \mathbb{R}_+$

$$f_{\text{blob},s_0}(x, y) = g_{2D}(x, y; s_0) = \frac{1}{2\pi s_0} e^{-\frac{x^2+y^2}{2s_0}} \quad (25)$$

will for both Laplacian and determinant of the Hessian interest point detection be equal to the size of the blob (Lindeberg 1998a, Equations (36) and (37)):

$$\begin{aligned} (\hat{x}, \hat{y}; \hat{s}) &= \operatorname{argmin}_{(x,y;s)} (\nabla_{\text{norm}}^2 L)(x, y; s) \\ &= (0, 0; s_0), \end{aligned} \quad (26)$$

$$\begin{aligned} (\hat{x}, \hat{y}; \hat{s}) &= \operatorname{argmax}_{(x,y;s)} (\det \mathcal{H}_{\text{norm}} L)(x, y; s) \\ &= (0, 0; s_0), \end{aligned} \quad (27)$$

– *edge detection* from combined

- maxima of the gradient magnitude in the spatial gradient direction e_v , reformulated such that the second-order directional derivative in the gradient direction L_{vv} is zero and the third-order directional derivative in the gradient direction L_{vvv} is negative (Lindeberg 1998b Equation (8)), and
- maxima over scale of the scale-normalised gradient magnitude $L_{v,\text{norm}}$ according to (Lindeberg 1998b Equation (15))

$$L_{v,\text{norm}} = s^{\gamma/2} \sqrt{L_x^2 + L_y^2}, \quad (28)$$

where we here set the scale normalisation parameter γ to (Lindeberg 1998b, Equation (23))

$$\gamma_{\text{edge}} = \frac{1}{2}, \quad (29)$$

such that the selected scale level \hat{s} for an idealised model of a diffuse edge (Lindeberg 1998b Equation (18))

$$\begin{aligned} f_{\text{edge},s_0}(x, y) &= \int_{u=-\infty}^x g_{1D}(u; s_0) du = \\ &= \int_{u=-\infty}^x \frac{1}{\sqrt{2\pi s_0}} e^{-\frac{u^2}{2s_0}} du \end{aligned} \quad (30)$$

will be equal to the amount of diffuseness $s_0 \in \mathbb{R}_+$ of that diffuse edge

$$\hat{s} = \operatorname{argmax}_s L_{v,\text{norm}}(0, 0; s) = s_0, \quad (31)$$

– *ridge detection* from combined

- zero-crossings of the first-order directional derivative L_p in the first principal curvature direction e_p of the Hessian matrix, such that $L_p = 0$ (Lindeberg 1998b Equations (42)), and

- minima over scale of the scale-normalised ridge strength in terms of the scale-normalised second-order derivative $L_{pp,\text{norm}}$ in the direction e_p according to (Lindeberg 1998b Equation (47)):

$$\begin{aligned} L_{pp,\text{norm}} &= s^\gamma L_{pp} = \\ &= s^\gamma \left(L_{xx} + L_{yy} - \sqrt{(L_{xx} - L_{yy})^2 + 4L_{xy}^2} \right), \end{aligned} \quad (32)$$

where we here choose the scale normalisation parameter γ as (Lindeberg 1998b, Equation (56))

$$\gamma_{\text{ridge}} = \frac{3}{4}, \quad (33)$$

such that the selected scale level \hat{s} for a Gaussian ridge model of the form

$$f_{\text{ridge},s_0}(x, y) = g_{1D}(x; s_0) = \frac{1}{\sqrt{2\pi s_0}} e^{-\frac{x^2}{2s_0}} \quad (34)$$

will be equal to the width $s_0 \in \mathbb{R}_+$ of that idealised ridge model

$$\hat{s} = \operatorname{argmax}_s L_{pp,\text{norm}}(0, 0; s) = s_0. \quad (35)$$

A common property of all these scale-invariant feature detectors is, thus, that the selected scale levels \hat{s} obtained from local extrema over scale will reflect characteristic¹ scales s_0 in the input data (Lindeberg 2021a). By evaluating discretisation methods of Gaussian derivatives with respect to such scale selection properties, we therefore have a way of formulating a well-defined proxy task, for evaluating how well the different types of discretisation methods lead to appropriate consistency properties over scales for the numerical implementations of Gaussian derivative operators.

Figures 6–9 in Appendix D provide visualisations of the conceptual steps involved when defining these scale estimates \hat{s} .

2.2.2 Quantitative measures for characterising the accuracy of the scale estimates obtained from the scale selection methodology

To quantify the performance of the different discretisation methods with regard to the above scale selection tasks, we will

- compute the selected scale levels $\hat{\sigma} = \sqrt{\hat{s}}$ for different values of the characteristic scale s_0 in the image data, measured in dimension length $\sigma_0 = \sqrt{s_0}$, and

¹ The notion of “characteristic scale” refers to a scale, that reflects a characteristic length in the image data, in a similar way as the notion of characteristic length is used in the areas of physics. See Appendix A.3.1 for further details.

- quantify the deviations from the reference in terms of the relative error measure (Lindeberg 2024 Equation (107))

$$E_{\text{scalest,rel}}(\sigma) = \frac{\hat{\sigma}}{\hat{\sigma}_{\text{ref}}} - 1, \quad (36)$$

under variations of the characteristic scale s_0 in the input image, where the deviations between the selected scale levels $\hat{\sigma} = \sqrt{\hat{s}}$ and the reference value $\sigma_0 = \sqrt{s_0}$ are to be interpreted as the results of discretisation errors.

When generating discrete model signals for the different discrete approximation methods, we use as conceptually close discretisation methods for the input model signals (Gaussian blobs for interest point detection, diffuse edges for edge detection, or Gaussian ridges for ridge detection) as for the discrete approximations of Gaussian derivatives, according to Appendix C.

3 Results

3.1 Characterisation of the effective amount of spatial smoothing in discrete approximations of Gaussian derivatives in terms of spatial spread measures

Figures 2–3 show the graphs of computing the spatial spread measure $\sqrt{V(|T_{x^\alpha}(\cdot; s)|)}$ according to (18) as well as the offset measure $O_\alpha(s)$ according to (20) over an interval of finer scale values $\sigma = \sqrt{s} \in [0.1, 2]$, for each one of the different discretisation methods described in Section 2.1.

As can be seen from these graphs:

- The agreement with the underlying fully continuous spread measures for the continuous Gaussian derivative kernels is substantially better for the genuinely sampled or integrated Gaussian derivative kernels than for the hybrid discretisations based on combining either the normalised sampled Gaussian kernel or the integrated Gaussian kernel with central difference operators.

In situations when multiple derivatives of different orders α are to be computed at the same scale levels, the hybrid discretisation methods are, however, as previously mentioned, computationally much more efficient, implying that the introduction of the hybrid discretisations implies a trade-off between the accuracy in terms of the overall amount of spatial smoothing of the equivalent discrete filters and the computational efficiency of the implementation.

- The agreement with the underlying fully continuous spread measures for the continuous Gaussian derivative kernels is substantially better for the genuinely discrete analogue of Gaussian derivative operators, obtained by first convolving the input data with the discrete analogue of the Gaussian kernel and then applying central difference operators to the spatially smoothing input data, compared to using any of the hybrid discretisations.

If, for efficiency reasons, a discretisation method is to be chosen, based on combining a first stage of spatial smoothing with a following application of central difference operators, the approach based on using spatial smoothing with the discrete analogue of the Gaussian kernel, in most of the cases, leads to better agreement with the underlying continuous theory, compared to using either the normalised sampled Gaussian kernel or the integrated Gaussian kernel in the first stage of spatial smoothing.

As previously stated, the hybrid discretisation methods may, however, anyway be warranted in situations where the underlying modified Bessel functions $I_n(s)$ are not fully available in the computational environment, where the discrete filtering operations are to be implemented, such as when performing learning of the scale levels in deep networks based on Gaussian derivative operators.

A further general implication of these results is that, depending on what discretisation method is chosen for discretising the computation of Gaussian derivative responses at fine scales, different values of the spatial scale parameter s will be needed, to obtain a comparable amount of spatial smoothing of the input data for the different discretisation methods.

3.2 Characterisation of the approximation properties relative to continuous scale space in terms of the scale levels selected by scale selection algorithms

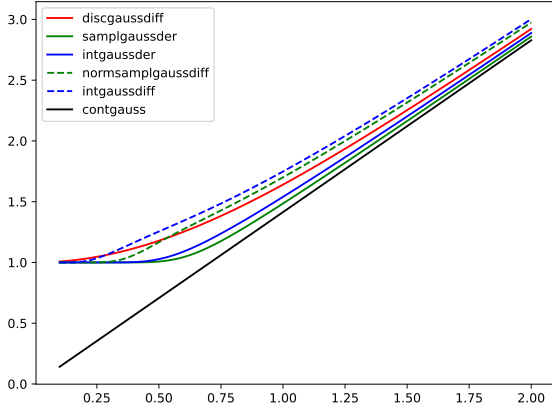
We will next characterise the approximation properties of the scale estimates for the different benchmark tasks outlined in Section 2.2.1 with regard to the quantitative measures defined in Section 2.2.2.

For generating the input data, we used 50 logarithmically scale values $\sigma_0 \in [1/3, 3]$. When performing the scale selection step, we searched over a range of 80 logarithmically scale levels $\sigma_0 \in [0.1, 5]$, and accumulated the variability over scale at the image center for each differential feature detector, and additionally performed parabolic interpolation over the logarithmic scale values, to localise the scale estimates to higher accuracy. This very dense sampling of the scale levels is far beyond what is usually needed in actual image processing or computer vision algorithms, but was chosen here in order to essentially eliminate the effects of discrete sampling issues in the scale direction.

Figure 4(a) shows a graph of the scale estimates obtained for the second-order Laplacian interest point detector in this way, with the corresponding relative scale errors in Figure 4(c). Figures 5(a) and 5(c) show corresponding results for the non-linear determinant of the Hessian interest point detector.

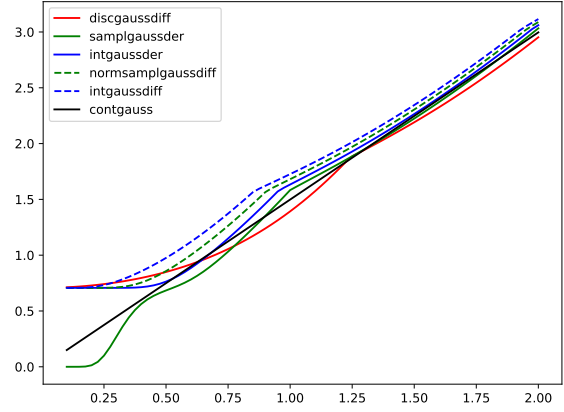
As can be seen from these graphs, the consistency errors in the scale estimates obtained for the hybrid discretisation

Spatial spread measures for 1st-order derivative kernels



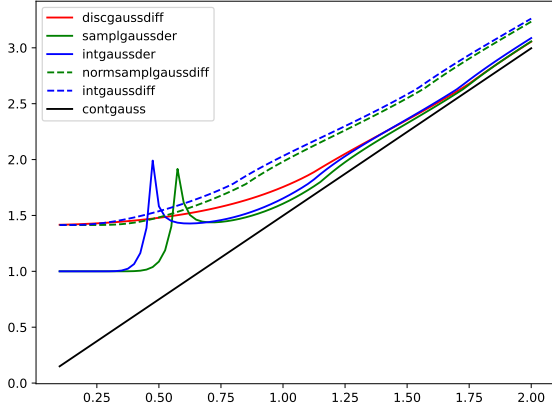
(a) Case: $\alpha = 1$. Note that the spatial spread measures for the spatial smoothing kernels combined with central differences are delimited from below by the spatial variance of the absolute value of the first-order central difference operator $|\delta_x|$, which is $\sqrt{V(|\delta_x|)} = 1$.

Spatial spread measures for 2nd-order derivative kernels



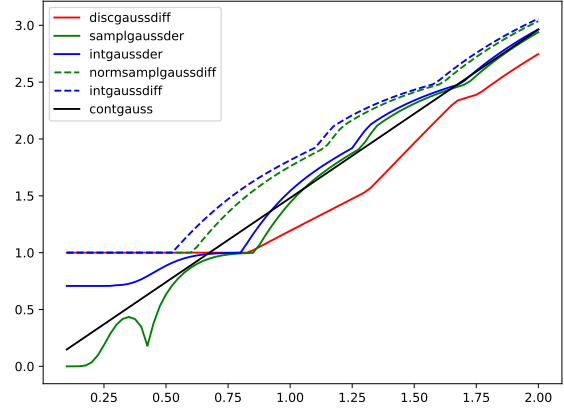
(b) Case: $\alpha = 2$. Note that the spatial spread measures for the spatial smoothing kernels combined with central differences are delimited from below by the spatial variance of the absolute value of the second-order central difference operator $|\delta_{xx}|$, which is $\sqrt{V(|\delta_{xx}|)} = 1/\sqrt{2}$.

Spatial spread measures for 3rd-order derivative kernels



(c) Case: $\alpha = 3$. Note that the spatial spread measures for the spatial smoothing kernels combined with central differences are delimited from below by the spatial variance of the absolute value of the third-order central difference operator $|\delta_{xxx}|$, which is $\sqrt{V(|\delta_{xxx}|)} = \sqrt{2}$.

Spatial spread measures for 4th-order derivative kernels



(d) Case: $\alpha = 4$. Note that the spatial spread measures for the spatial smoothing kernels combined with central differences are delimited from below by the spatial variance of the absolute value of the fourth-order central difference operator $|\delta_{xxxx}|$, which is $\sqrt{V(|\delta_{xxxx}|)} = 1$.

Fig. 2: Graphs of the *spatial spread measure* $\sqrt{V(|T_{x^\alpha}(\cdot; s)|)}$ according to (18) for different discrete approximations of Gaussian derivative kernels of order α : **(i)** for either discrete analogues of Gaussian derivative kernels $T_{\text{disc},x^\alpha}(n; s)$ according to (10), corresponding to convolutions with the discrete analogue of the Gaussian kernel $T_{\text{disc}}(n; s)$ according to (7) followed by central differences according to (13), **(ii)** sampled Gaussian derivative kernels $T_{\text{sampl},x^\alpha}(n; s)$ according to (8), **(iii)** integrated Gaussian derivative kernels $T_{\text{int},x^\alpha}(n; s)$ according to (9), **(iv)** the hybrid discretisation kernel $T_{\text{hybr-sampl},x^\alpha}(n; s)$ according to (16), corresponding to convolution with the normalised sampled Gaussian kernel $T_{\text{normsampl}}(n; s)$ according to (5) followed by central differences according to (13), and **(v)** the hybrid discretisation kernel $T_{\text{hybr-int},x^\alpha}(n; s)$ according to (17), corresponding to convolution with the integrated Gaussian kernel $T_{\text{int}}(n; s)$ according to (6) followed by central differences according to (13). (**Horizontal axes:** Scale parameter in units of $\sigma = \sqrt{s} \in [0.1, 2]$.)

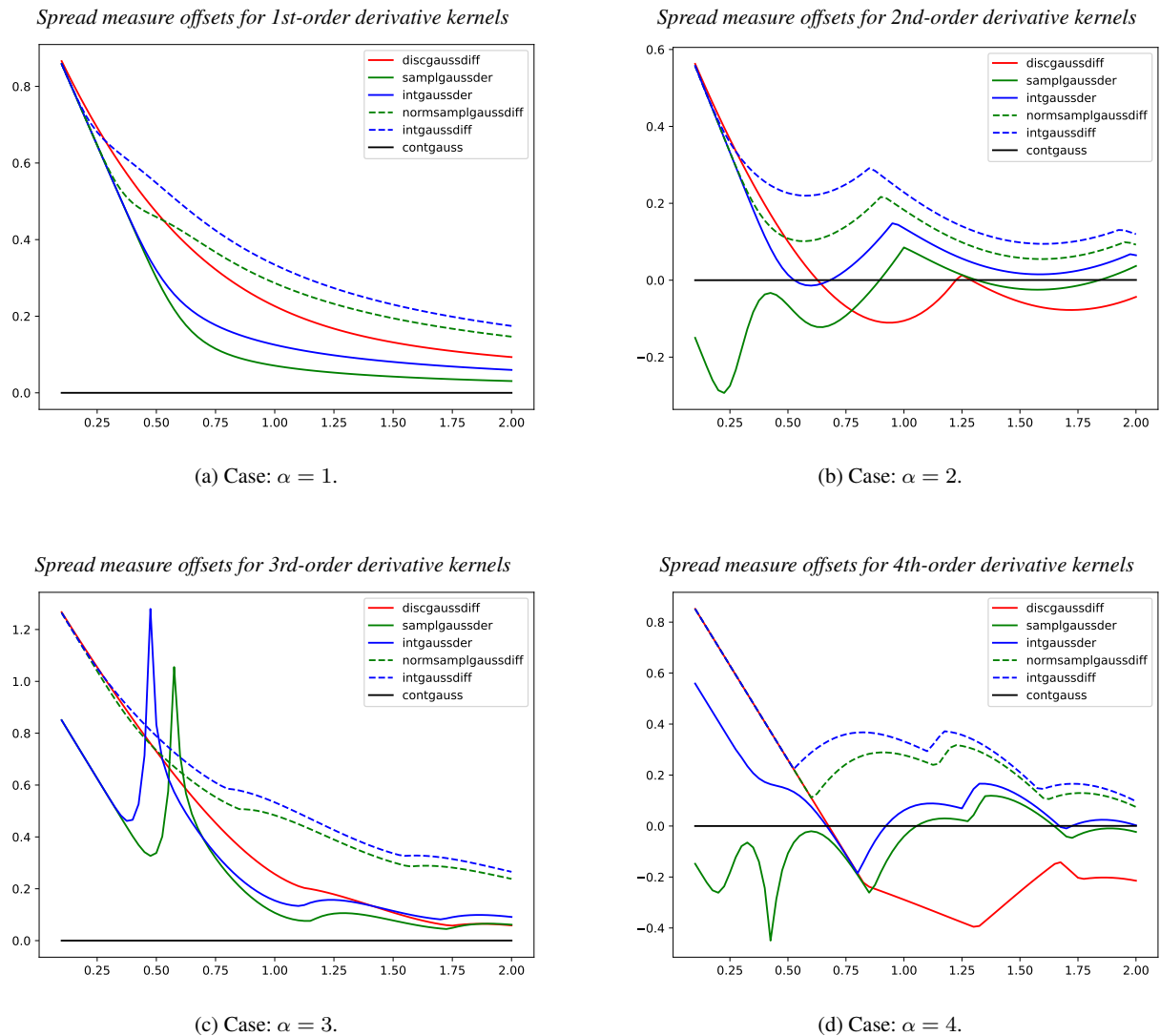


Fig. 3: Graphs of the *spatial spread measure offset* $O_\alpha(s)$, relative to the spatial spread of a continuous Gaussian kernel, according to (20), for different discrete approximations of Gaussian derivative kernels of order α : **(i)** for either discrete analogues of Gaussian derivative kernels $T_{\text{disc},x^\alpha}(n; s)$ according to (10), corresponding to convolutions with the discrete analogue of the Gaussian kernel $T_{\text{disc}}(n; s)$ according to (7) followed by central differences according to (13), **(ii)** sampled Gaussian derivative kernels $T_{\text{sampl},x^\alpha}(n; s)$ according to (8), **(iii)** integrated Gaussian derivative kernels $T_{\text{int},x^\alpha}(n; s)$ according to (9), **(iv)** the hybrid discretisation kernel $T_{\text{hybr-sampl},x^\alpha}(n; s)$ according to (16), corresponding to convolution with the normalised sampled Gaussian kernel $T_{\text{normsampl}}(n; s)$ according to (5) followed by central differences according to (13), and **(v)** the hybrid discretisation kernel $T_{\text{hybr-int},x^\alpha}(n; s)$ according to (17), corresponding to convolution with the integrated Gaussian kernel $T_{\text{int}}(n; s)$ according to (6) followed by central differences according to (13). (**Horizontal axes:** Scale parameter in units of $\sigma = \sqrt{s} \in [0.1, 2]$.)

methods, based on either the normalised Gaussian kernel or the integrated Gaussian kernel with central differences, are for larger values of the scale parameter higher than the corresponding consistency errors in the regular discretisation methods based on either sampled Gaussian derivatives or integrated Gaussian derivatives. For smaller values of the scale parameter, there is, however, a range of scale values, where the consistency errors are lower for the hybrid discretisation methods than for underlying corresponding regular discretisation methods.

Notably, the consistency errors for the discretisation methods involving central differences are also generally lower for the genuinely discrete method, based on convolution with the discrete analogue of the Gaussian kernel followed by central differences, than for the hybrid methods.

Figure 4(b) shows the selected scale levels for the first-order gradient-magnitude-based edge detection operation, with the corresponding relative error measures shown in Figure 4(d). As can be seen from these graphs, the consistency errors are notably higher for the hybrid discretisation approaches, compared to their underlying regular methods. In these ex-

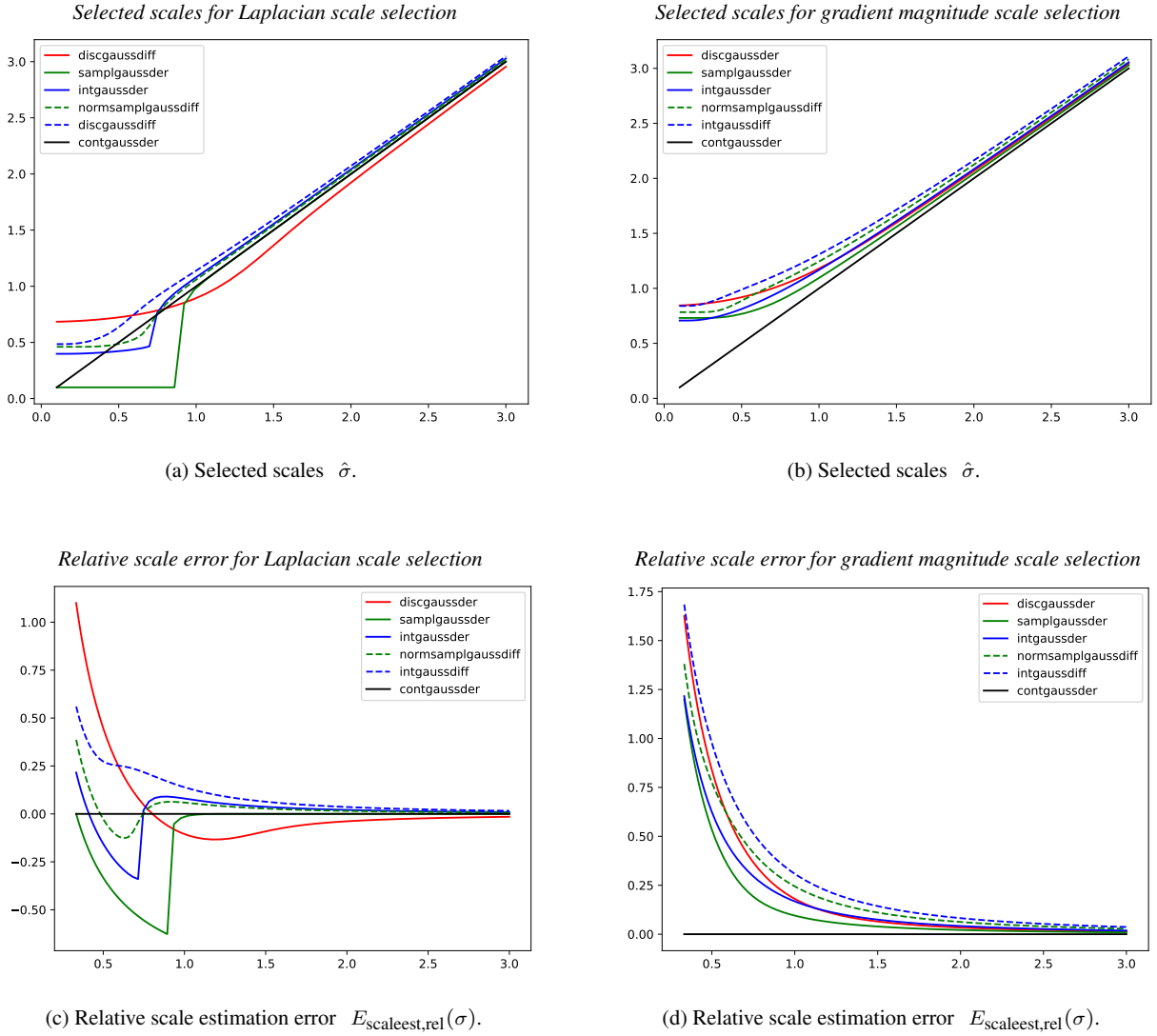


Fig. 4: Graphs of the *selected scales* $\hat{\sigma} = \sqrt{\hat{s}}$ as well as the *relative scale estimation error* $E_{\text{scaleest,rel}}(\sigma)$, according to (36), when **(left column)** applying scale selection from local extrema over scale of the *scale-normalised Laplacian* response according to (23) to a set of Gaussian blobs of different size $\sigma_{\text{ref}} = \sigma_0$, for different discrete approximations of the Gaussian derivative kernels or **(right column)** when applying scale selection from local extrema over scale of the *scale-normalised gradient magnitude* response according to (28) to a set of diffuse step edges of different width $\sigma_{\text{ref}} = \sigma_0$, for either **(i)** discrete analogues of Gaussian derivative kernels $T_{\text{disc},x^\alpha}(n; s)$ according to (10), **(ii)** sampled Gaussian derivative kernels $T_{\text{sampl},x^\alpha}(n; s)$ according to (8), **(iii)** integrated Gaussian derivative kernels $T_{\text{int},x^\alpha}(n; s)$ according to (9), **(iv)** the hybrid discretisation method corresponding the equivalent convolution kernels $T_{\text{hybr-sampl},x^\alpha}(n; s)$ according to (16) or **(v)** the hybrid discretisation method corresponding the equivalent convolution kernels $T_{\text{hybr-int},x^\alpha}(n; s)$ according to (17). (**Horizontal axes:** Reference scale $\sigma_{\text{ref}} = \sigma_0 \in [1/3, 3]$.)

periments, the consistency errors are also higher for the hybrid discretisation methods than for the genuinely discrete approach, based on discrete analogues of Gaussian derivatives.

Finally, Figures 5(b) and 5(d) show corresponding results for the second-order principal-curvature-based ridge detector, which are structurally similar to the previous results for the second-order Laplacian and determinant of the Hessian interest point detectors.

4 Summary and discussion

In this paper, we have extended the in-depth treatment of different discretisations of Gaussian derivative operators in terms of explicit convolution operations in (Lindeberg 2024) to two more discretisation methods, based on hybrid combinations of either convolutions with normalised sampled Gaussian kernels or convolutions with integrated Gaussian kernels with central difference operators.

The results from the treatment show that it is possible to characterise general properties of these hybrid discretisation

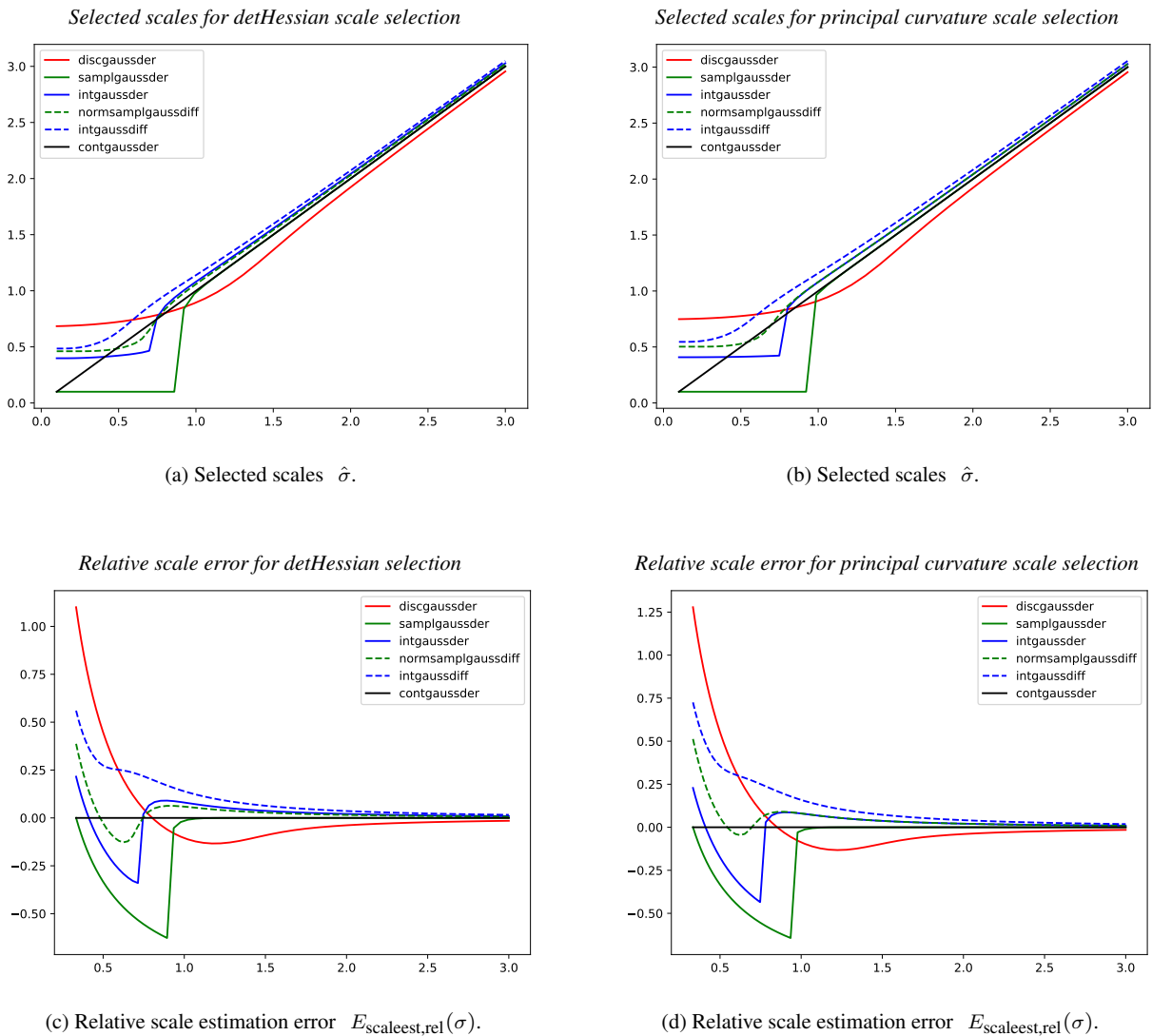


Fig. 5: Graphs of the *selected scales* $\hat{\sigma} = \sqrt{\hat{s}}$ as well as the *relative scale estimation error* $E_{\text{scaleest,rel}}(\sigma)$, according to (34) when **(left column)** applying scale selection from local extrema over scale of the *scale-normalised determinant of Hessian* response according to (22) to a set of Gaussian blobs of different size $\sigma_{\text{ref}} = \sigma_0$, for different discrete approximations of the Gaussian derivative kernels or **(right column)** when applying scale selection from local extrema over scale of the *scale-normalised principal curvature* response according to (30) to a set of Gaussian ridges of different width $\sigma_{\text{ref}} = \sigma_0$, for either **(i)** discrete analogues of Gaussian derivative kernels $T_{\text{disc},x^\alpha}(n; s)$ according to (10), **(ii)** sampled Gaussian derivative kernels $T_{\text{sampl},x^\alpha}(n; s)$ according to (8), **(iii)** integrated Gaussian derivative kernels $T_{\text{int},x^\alpha}(n; s)$ according to (9), **(iv)** the hybrid discretisation method corresponding the equivalent convolution kernels $T_{\text{hybr-sampl},x^\alpha}(n; s)$ according to (16) or **(v)** the hybrid discretisation method corresponding the equivalent convolution kernels $T_{\text{hybr-int},x^\alpha}(n; s)$ according to (17). **(Horizontal axes:** Reference scale $\sigma_{\text{ref}} = \sigma_0 \in [1/3, 3]$.)

methods in terms of the effective amount of spatial smoothing that they imply. Specifically, for very small values of the scale parameter, the results obtained after the spatial discretisation may differ significantly from the results obtained from the fully continuous scale-space theory, as well as between the different types of discretisation methods.

The results from this treatment are intended to be generically applicable in situations, when scale-space operations are to be applied at scale levels below the otherwise rule of thumb in classical computer vision, of not going below a certain minimum scale level, corresponding to a standard

deviation of the Gaussian kernel of the order of $1/\sqrt{2}$ or 1. We argue that the presented quantitative performance characterisations should have a predictive ability, for how the different types of discrete derivative approximation methods could have comparative advantages in other multi-scale settings.

One direct application domain for these results is when implementing deep networks in terms of Gaussian derivatives, where empirical evidence indicates that deep networks often tend to benefit from using finer scale levels than as in-

licated by the previous rule of thumb in classical computer vision, and which we will address in future work.

Acknowledgments

Python code, that implements the discretisation methods for Gaussian smoothing and Gaussian derivatives in this paper, is available in the `pyscsp` package, available at GitHub:

`https://github.com/tonylindeberg/pyscsp`

as well as through PyPi:

`pip install pyscsp`

Appendix

A Theoretical background of the notion of scale-space representation

Concerning the notion of multi-scale signal and image representations, the concept of scale-space representation stands out as a canonical type of multi-scale representation, in the respect that its basic image operators in terms of Gaussian smoothing and Gaussian derivatives can be *uniquely* determined from symmetry properties that reflect structural properties of the environment in combination with requirements to guarantee consistent treatment of image structures between different spatial scales (Iijima 1962; Koenderink 1984; Koenderink and van Doorn 1992; Lindeberg 1996, 2011, 2021b; Weickert *et al.* 1999).

This appendix section develops the basic theoretical background concerning scale-space representation, regarding:

- the definitions of a scale-space representation with its Gaussian derivative responses,
- the fundamental scale covariance property of the scale-normalised Gaussian derivative responses and homogeneous polynomial differential invariants constructed from scale-normalised Gaussian derivative responses,

which are then used in Sections 2.2 and 3.2 for:

- quantifying the performance of different discrete approximations of Gaussian in terms of scale selection properties for different types of differential feature detectors.

Compared to previous presentations of these topics, mainly devoted to 2-D images, and which this presentation builds upon, the treatment in this section is performed for general D -dimensional images. Note specifically that in order to handle the general D -dimensional case in this supplementary appendix, we throughout refer denote the D -dimensional image coordinates as $x = (x_1, x_2, \dots, x_D)^T$ as opposed to as the use of (x, y) for the 2-D image coordinates in Section 2.2.

A.1 Scale-space representation and Gaussian derivative responses

Given a D -dimensional signal $f: \mathbb{R} \rightarrow \mathbb{R}$, a scale-space representation $L: \mathbb{R} \times \mathbb{R}_+ \rightarrow \mathbb{R}$ is the one-parameter family of signals obtained by convolving the input signal

$$L(x; s) = (g(\cdot; s) * f(\cdot))(x; s) = \int_{u \in \mathbb{R}^D} f(x-u) g(u; s) du \quad (37)$$

with D -dimensional Gaussian kernels at different scales $s \in \mathbb{R}_+$

$$g(x; s) = \frac{1}{\sqrt{2\pi s}^D} e^{-\frac{x^T x}{2s}}, \quad (38)$$

where $x = (x_1, x_2, \dots, x_D)^T$ denotes D -dimensional image coordinates.

From this representation, Gaussian derivative responses of order α , where $\alpha = (\alpha_1, \alpha_2, \dots, \alpha_D)$ is a multi-index notation, are, in turn, defined as

$$L_{x^\alpha}(x; s) = \partial_{x^\alpha} L(x; s) = (g_{x^\alpha}(\cdot; s) * f(\cdot))(x; s), \quad (39)$$

where

$$g_{x^\alpha}(x; s) = \partial_{x^\alpha} (g(x; s)) = \partial_{x_1^{\alpha_1} x_2^{\alpha_2} \dots x_D^{\alpha_D}} (g(x; s)) \quad (40)$$

denotes the D -dimensional Gaussian derivative kernel of order α . In the area of scale-space theory for image processing and computer vision, it has been shown that such Gaussian derivative responses can be used as a powerful basis for expressing a large number of visual operations, including feature detection, image matching, classification and object recognition, see Lindeberg (1994, 1999, 2008) for overviews.

A.2 Scale covariance property of Gaussian derivative responses

With regard to handling image structures at different spatial scales, a very useful property of this notion of scale-space representation is that it is closed under spatial scaling transformations of the form

$$f'(x') = f(x) \quad \text{for} \quad x' = Sx, \quad (41)$$

where $S > 0$ is a spatial scaling factor. Specifically, if we define scale-normalised Gaussian derivative responses according to (Lindeberg 1998a Equation (18))

$$L_{\xi^\alpha}(x; s) = s^{|\alpha|/2} L_{x^\alpha}(x; s), \quad (42)$$

where $\gamma > 0$ is a scale normalisation power and $|\alpha| = \alpha_1 + \alpha_2 + \dots + \alpha_D$ denotes the total order of differentiation, then it follows that if we additionally define the scale-normalised Gaussian derivative response of the rescaled signal $f'(x')$ according to

$$L'_{x^\alpha}(x'; s') = (s'^{\gamma|\alpha|/2} g_{x^\alpha}(\cdot; s') * f'(\cdot))(x'; s'), \quad (43)$$

then the corresponding scale-normalised responses between matching image positions x and x' in the two domains will be equal up to a uniform scaling factor (see Lindeberg (1998a) Equation (20), although with different notation for the scale parameters and the scaling factor used there)

$$L_{x^\alpha}(x; s) = S^{|\alpha|(1-\gamma)} L'_{x^\alpha}(x'; s'), \quad (44)$$

provided that the values of the scale parameters s and s' in the two domains are matched according to

$$s' = S^2 s. \quad (45)$$

This scale covariance property of Gaussian derivative responses has been of fundamental importance to classical computer vision, for formulating scale-invariant algorithms that can handle *a priori* unknown scaling variabilities in image data in a fully automatic manner (Lindeberg 1998a, 1998b, 2013a, 2015, 2021a; Bretzner and Lindeberg 1998; Chomat *et al.* 2000; Lowe 2004; Bay *et al.* 2008). When using Gaussian derivative responses as mathematical primitives for formulating the layers in deep networks, this scale covariance property has

also been of fundamental importance for formulating provably scale-covariant and scale-invariant deep networks (Lindeberg 2020, 2022; Sangalli *et al.* 2022; Yang *et al.* 2023).

Specifically, with regard to feature detection methods formulated in terms of homogeneous polynomial combinations of such scale-normalised Gaussian derivative responses (Lindeberg 1998a Equation (21))

$$(\mathcal{D}_{\text{norm}}L)(x; s) = \sum_{i=1}^I c_i \prod_{j=1}^J L_{\xi^{\alpha_{ij}}}(x; s) \quad (46)$$

where the sum of the orders of differentiation in a certain term

$$\sum_{j=1}^J |\alpha_{ij}| = M \quad (47)$$

is the same for all the terms in (46) with indices i , then the corresponding transformed feature

$$(\mathcal{D}_{\text{norm}}L')(x'; s') = \sum_{i=1}^I c_i \prod_{j=1}^J L'_{\xi^{\alpha_{ij}}}(x'; s') \quad (48)$$

will for matching spatial positions x and x' be equal up to a uniform scaling factor (see Lindeberg (1998a) Equation (25), although again with different notation of the spatial scale parameters and the spatial scaling factor used there)

$$(\mathcal{D}_{\text{norm}}L)(x; s) = S^{M(1-\gamma)}(\mathcal{D}_{\text{norm}}L')(x'; s'), \quad (49)$$

provided that the scale parameters s and s' are matched according to (45).

Examples of such scale-normalised differential feature detectors for the case of 2-D spatial images are given in Equations (23) and (24) regarding interest point detection, in Equation (28) regarding edge detection and in Equation (32) regarding ridge detection.

A.3 Evaluating discretisation methods based on consistency requirement relative to scale selection properties

In the experiments reported in Section 3, we use consistency measurements relative to this transformation property of Gaussian-derivative-based feature detectors under spatial scaling transformations, to quantitatively evaluate to quality of different discrete approximations of Gaussian derivative kernels, that are used for approximating Gaussian derivative responses in discrete implementations for 2-D image data.

Specifically, we will evaluate feature detectors in terms of interest point detection, edge detection and ridge detection, formulated with the systematic scale selection methodology proposed in (Lindeberg 1998a, 1998b), based on detecting local extrema over scales of scale-normalised differential entities of the form (46) according to

$$\{\hat{s}(x)\} = \text{argmaxminlocal}_s(\mathcal{D}_{\text{norm}}L)(x; s), \quad (50)$$

where $\text{argmaxminlocal}_s(\mathcal{D}_{\text{norm}}L)(x; s)$ denotes the set of all local extrema over scale of the differential entity $\mathcal{D}_{\text{norm}}L$ at the spatial point x . In the ideal continuous case, it holds that these scale levels \hat{s} , where local extrema of differential invariants of the form (46) assume local maxima over scales, will transform according to (45)

$$\hat{s}' = S^2 \hat{s}, \quad (51)$$

and are in this respect provably scale covariant.

Due to deviations between the continuous theory and the discrete implementation, based on spatially discretised input functions combined with different spatial discretisations of the Gaussian derivative

kernels, we cannot, however, expect corresponding properties to hold exactly in a numerical implementation. In this respect, the deviations between the results obtained from a discrete implementation of these computational steps in relation to the corresponding fully continuous results can be used for evaluating the approximation properties of different approaches for discretising Gaussian derivative operators.

With such a paradigm for quantitative evaluation, we can, in particular, quantify the accuracy of different spatial discretisations relative to a primary desirable property of a multi-scale representation.

In methods for feature detection with automatic scale selection, it is specifically assumed that the scale levels \hat{s} , where appropriately designed differential feature detectors assume their maxima over scales, may correspond to interesting structures in the original image data. By experimental investigations for different types of feature detectors, for tasks such as edge detection, blob detection, corner detection, interest point detection and dense local scale estimation, it has been demonstrated that this approach allows for robust feature detectors that very well handle substantial variabilities in scale for natural image data (Lindeberg 1998a, 1998b, 1999, 2013a, 2018, 2021a; Lowe 2004).

A.3.1 The notion of characteristic scale

In the area of computer vision, such locally dominant scale values in the image data, where scale-normalised differential entities assume local extrema over scale, are often referred to as locally “characteristic scales”, based on the empirically verified hypothesis that such scale levels, when measured in terms of the scale parameter expressed in units dimension of [length] as $\sigma = \sqrt{s}$, will for both idealised models of image structures and natural image data with similar appearance reflect a characteristic length of such image structures. See the introduction of Section 4 in (Lindeberg 1998a) for a definition of the notion of characteristic length of features extracted image data and more generally Sections 5.1 and 6.2 in (Lindeberg 1998a), Sections 4.5 and 5.6.1 in (Lindeberg 1998b), Sections 3.1.1 and 3.2–3.3 in (Lindeberg 2013a) and Sections 2.2–2.3 in (Lindeberg 2018) for examples of mathematical analysis of scale selection properties for different types of idealised model signals.

B Theoretical background for discretisations of the Gaussian smoothing operation and the Gaussian derivative operators

This section gives mathematical definitions of the different discretisation methods, that we will consider for discrete approximations of Gaussian derivative operators and then quantitatively evaluate in Section 3. For simplicity, we throughout restrict ourselves to convolution operations that are separable over the D -dimensional image data, thereby making it possible to restrict the following theoretical treatment to studying 1-D discrete approximations of Gaussian derivatives, based on the separability property of the Gaussian derivative operators in the continuous case described below.

The theoretical material in this appendix is based on an in-depth treatment of the topic of approximating the Gaussian convolution and the Gaussian derivative operators for discrete data in (Lindeberg 2024). For related treatments of the topic of approximating scale-space operators on discrete data, see also (Lindeberg 1990, 1993b, 1993a, Åström and Heyden 1997, Wang 1999, Lim and Stiehl 2003, Tschirsich and Kuijper 2015, Slavík and Stehlík 2015, Rey-Otero and Delbracio 2016).

B.1 Separable Gaussian smoothing and Gaussian derivative computations

Due to the separability of the Gaussian kernel in Equation (38)

$$g(x; s) = \prod_{i=1}^D g_{1D}(x_i; s), \quad (52)$$

where $g_{1D}(x_i; s)$ denotes a 1-D Gaussian kernel over the i :th dimension with $x = (x_1, \dots, x_D)$

$$g_{1D}(x_i; s) = \frac{1}{\sqrt{2\pi s}} e^{-\frac{x_i^2}{2s}}, \quad (53)$$

it follows that the D -dimensional convolution integral for computing the D -dimensional scale-space representation according to (37) can be computed as a cascade of separable Gaussian convolution steps

$$L(x; s) = \int_{u_1 \in \mathbb{R}} g_{1D}(u_1; s) \dots \left(\int_{u_D \in \mathbb{R}} g_{1D}(u_D; s) f(x_1 - u_1, \dots, x_D - u_D) du_D \right) \dots du_1. \quad (54)$$

In a corresponding way, from the separability of the corresponding Gaussian convolution kernels with $\alpha = (\alpha_1, \dots, \alpha_D)$

$$g_{x^\alpha}(x; s) = \prod_{i=1}^D g_{1D, x^{\alpha_i}}(x_i; s), \quad (55)$$

where each 1-D Gaussian derivative kernel is given by

$$g_{1D, x^{\alpha_i}}(x_i; s) = \partial_{x_i^{\alpha_i}}(g_{1D}(x_i; s)), \quad (56)$$

it follows that the D -dimensional Gaussian derivative kernel of order α can be computed with a separable cascade with a set of 1-D Gaussian derivative kernels of order α_i along each of the respective dimensions according to

$$L_{x^\alpha}(x; s) = \int_{u_1 \in \mathbb{R}} g_{1D, x^{\alpha_1}}(u_1; s) \dots \left(\int_{u_D \in \mathbb{R}} g_{1D, x^{\alpha_D}}(u_D; s) f(x_1 - u_1, \dots, x_D - u_D) du_D \right) \dots du_1. \quad (57)$$

B.2 Definition of the 1-D modelling problems studied regarding discrete approximations of Gaussian smoothing and Gaussian derivatives

In the following, we will henceforth² consider spatial discretisations of 1-D Gaussian convolution integrals of the form

$$L(x; s) = \int_{u \in \mathbb{R}} g_{1D}(u; s) f(x - u) du \quad (58)$$

² In fact, for the principled axiomatic theory of discrete scale-space representations in (Lindeberg 1990, 1993a), it has been shown that more accurate approximations to rotational symmetry can be obtained by instead using discrete kernels that are not formally restricted to being computed with a cascade of only using one convolution kernel along each dimension (Lindeberg 1993a Proposition 4.16). Since those more isotropic discretisations, however, require either the combination of two separable convolutions along the Cartesian coordinate

with discrete approximations of Gaussian kernels of the form

$$L(x; s) = \sum_{n \in \mathbb{Z}} T(n; s) f(x - n), \quad (59)$$

as well as spatial discretisations of 1-D Gaussian derivative convolution integrals of the form

$$L_{x^\alpha}(x; s) = \int_{u \in \mathbb{R}} g_{1D, x^\alpha}(u; s) f(x - u) du \quad (60)$$

with discrete approximations of Gaussian derivative kernels of the form

$$L_{x^\alpha}(x; s) = \sum_{n \in \mathbb{R}} T_{x^\alpha}(n; s) f(x - n), \quad (61)$$

where we will then specifically consider different options for choosing the discrete approximations of Gaussian kernels $T(n; s)$ and the discrete approximations of Gaussian derivative kernels $T_{x^\alpha}(n; s)$, or mathematical equivalent formulations thereof, based on different types of criteria.

B.3 The sampled Gaussian kernel

The presumably most straightforward approach to approximate the continuous Gaussian convolution integral (58) by a discrete convolution operation of the form (59) is by sampling the continuous integral (58) with equidistant samples, which then corresponds to discrete convolution with the sampled Gaussian kernel

$$T_{\text{sampl}}(n; s) = g_{1D}(n; s) \quad (62)$$

with the sampled Gaussian kernel $g_{1D}(n; s)$ defined from the corresponding continuous kernel $g_{1D}(x; s)$ according to (53).

While this operation can be expected to work very well for sufficiently large values of the scale parameter s , this operation may, however, imply potential problems for very small values of the scale parameter. As developed further in (Lindeberg 2024 Section 2.3), for very small values of the scale parameter s , the sum of the discrete filter coefficients may significantly exceed 1, which implies that the corresponding discrete convolution operation then cannot be regarded as a true spatial smoothing process, since it will not leave a constant signal essentially unchanged. For this reason, it is therefore natural to consider using other types of discretisation method for discretising the Gaussian convolution integral at very fine scales.

B.4 The normalised sampled Gaussian kernel

A straightforward, but *ad hoc*, way of avoiding that the sum of the filter coefficients may exceed 1 is by instead normalizing the filter coefficient in the sampled Gaussian kernel to unit l_1 -norm

$$T_{\text{normsampl}}(n; s) = \frac{g(n; s)}{\sum_{m \in \mathbb{Z}} g(m; s)}. \quad (63)$$

Then, we are sure that a constant input signal is left unchanged. Still, however, a potential problem that arises when to use the resulting normalised sampled Gaussian kernel for discrete implementation is that

directions with two separable diagonal convolutions in the 2-D case, or a Fourier-based implementation, and we are for our intended applications interested in achieving high computational efficiency with publicly available software libraries for discrete implementations based on purely discrete convolution operations, we will, however, not consider those discretisations in this work.

the discrete variance of the resulting discrete sampled Gaussian kernel may for small values of the scale parameter be significantly lower than the continuous variance of the continuous Gaussian kernel (see Lindeberg (2024) Section 2.4, specifically Figures 3–4 in that paper for additional details). Since the variance of a kernel is not affected by a renormalisation of the filter coefficients, the same structural problem applies also to the regular sampled Gaussian kernel $T_{\text{sampl}}(n; s)$.

B.5 The integrated Gaussian kernel

A possibly less *ad hoc* way, of avoiding that the sum of the discrete filter coefficients could deviate from their aimed ideal value 1, is by instead forming a discrete approximation of the Gaussian kernel by integrating the values of the continuous Gaussian kernel over each pixel support region

$$T_{\text{int}}(n; s) = \int_{x=n-1/2}^{n+1/2} g(x; s) dx. \quad (64)$$

Then, it clearly follows that the sum of the filter coefficient in the resulting discrete kernel will be guaranteed to be equal to 1. As further described in (Lindeberg 2024 Section 2.5 and Appendix A.2), the effect of this approach is equivalent to first defining a continuous input function $f_c(x)$, that over each pixel support region is equal to the integral of the original function $f(x)$ over that pixel support region, and then subjecting that continuous signal $f_c(x)$ to continuous Gaussian convolution. As further described in (Lindeberg 2024 Section 2.5), the spatial integration operation in the definition of the derived continuous signal $f_c(x)$ from the original input signal $f(x)$ does, however, introduce a scale bias, in the sense that the discrete variance of the integrated Gaussian kernel may be significantly larger than the continuous variance of the continuous Gaussian kernel.

B.6 The discrete analogue of the Gaussian kernel

A more principled approach to defining a discrete approximation of the Gaussian kernel is by instead formulating similar assumptions (referred to as scale-space axioms in the area of scale-space theory) over a discrete domain as uniquely single out the choice of the continuous Gaussian kernel over a continuous domain.

In (Lindeberg 1990, 1993a) it is shown that, if we assume that (i) the discrete kernels should be guaranteed to not never introduce new local extrema or equivalently new zero-crossings from any finer to any coarser level of scale, then if combined with (ii) a semi-group property

$$T(\cdot; s_1) * T(\cdot; s_2) = T(\cdot; s_1 + s_2) \quad (65)$$

(iii) spatial symmetry through the origin $T(-n; s) = T(n; s)$, and (iv) normalisation to unit l_1 norm $\sum_n T(n; s) = 1$, then the special family of kernels

$$T_{\text{disc}}(n; s) = e^{-s} I_n(s), \quad (66)$$

referred to as the discrete analogue of the Gaussian kernel is singled out *uniquely*, where $I_n(s)$ denotes the modified Bessel functions of integer order. This discrete kernel $T_{\text{disc}}(n; s)$ is specifically the natural heat kernel over a 1-D discrete domain, in the respect that it satisfies the semi-discrete diffusion equation

$$\partial_s L = \frac{1}{2} \delta_{xx} L \quad (67)$$

with initial condition $L(n; 0) = f(n)$, where δ_{xx} denotes the second-order discrete difference operator $\delta_{xx} = (+1, -2, +1)$.

With regard to handling multiple spatial scales in signals, an additional attractive property of this discrete kernel is that the discrete variance of the discrete analogue of the Gaussian kernel is exactly equal to the value of the scale parameter

$$V(T(\cdot; s)) = \sum_{n \in \mathbb{Z}} n^2 T(n; s) = s. \quad (68)$$

In this respect, this discrete analogue of the Gaussian kernel conceptually avoids the structural problems with the sampled Gaussian kernel and the normalised sampled Gaussian kernel at very fine scales, as described in Sections B.3 and B.4 above. Additionally, the discrete analogue of the Gaussian kernel also avoids the scale offset of the integrated Gaussian kernel, as described in Section B.5 above.

B.7 The sampled Gaussian derivative kernel

In analogy with the definition of the sampled Gaussian kernel in Section B.3 above, the presumably most straightforward approach of approximating the Gaussian derivative convolution integral (61) is by sampling that convolution integral with equidistant samples, which then directly leads to a convolution with the sampled Gaussian derivative kernel

$$T_{\text{sampl}, x^\alpha}(n; s) = g_{x^\alpha}(n; s). \quad (69)$$

As for the previously mentioned problems regarding the sampled Gaussian kernel, as described in Section B.3 above, a conceptual problem with the sampled Gaussian derivative kernel, however, is that that sampling process may lead to substantial discretisation artefacts at very fine scales, which then, as previously described in (Lindeberg 2024 Section 3.3, specifically Figures 10–11 in that paper), implies that the discrete variance of (the absolute value of) the sampled Gaussian derivative kernel may vary significantly from the continuous variance of (the absolute value of) the continuous Gaussian kernel. Due to this property, the value of the scale parameter s may not fully reflect the amount of discrete blur in the corresponding discrete derivative approximation kernel at very fine scales.

Another practical computational problem, that arises with the sampled Gaussian derivative approach, is furthermore that in use cases, where multiple derivatives of different orders α are to be computed from the same input signal f , then the computation of each discrete approximation of the Gaussian derivative response for each order requires a new discrete convolution operation with a full size discrete derivative approximation kernel. Thereby, the computational work increases linearly, with the same factor, for increasing numbers of orders of differentiation, which can be problem in situations where very large numbers of Gaussian derivative responses are to be computed, such as in the application of Gaussian derivative operators as computational primitives in deep networks.

For these reasons, it is therefore warranted to also consider other types of discretisation methods for computing discrete approximations of Gaussian derivative responses.

B.8 The integrated Gaussian derivative kernel

In analogy with the definition of the integrated Gaussian kernel in Section B.5 above, we can also with the potential aim of trying to reduce the severe discretisation artefacts of the sampled Gaussian kernel at very fine scales, define an integrated Gaussian kernel by integrating the values of the continuous Gaussian derivative kernel over each pixel support region

$$T_{\text{int}, x^\alpha}(n; s) = \int_{x=n-1/2}^{n+1/2} g_{x^\alpha}(x; s) dx. \quad (70)$$

As described in (Lindeberg 2024 Section 3.4 and Appendix A.2), the effect of this operation is equivalent to first defining a continuous input signal $f_c(x)$, by integrating the original input signal $f(x)$ over each pixel support region and then letting the new continuous input signal $f_c(x)$ be equal to that average value over each pixel support region. As further described in (Lindeberg 2024 Section 3.4, specifically Figures 10–11 in that paper), a problem with this approach is, however, is that the spatial integration operation, used for defining the new continuous input signal $f_c(x)$ from the original input signal $f(x)$, introduces a scale bias.

When to use the integrated Gaussian derivative kernel for computing discrete approximations of multiple orders, this approach also suffers from the same problem as the sampled Gaussian derivative kernel, as described in Section B.7 above, in that a new large support convolution operation needs to be invoked for each order of differentiation, thus implying that the computational work will increase with the same linear factor for increasing numbers of orders of differentiation, which may be a substantial problem in situations when a very large number of Gaussian derivative responses are to be computed, such as in deep networks based on using combinations of Gaussian derivative operators as the computational primitives.

B.9 Discrete derivative approximations constructed from the combination of the discrete analogue of the Gaussian kernel with central differences

According to the theory for discrete derivative approximations with scale-space properties in (Lindeberg 1993b, 1993a) (see also Lindeberg (2024) Section 3.5), discrete approximations of Gaussian derivative responses can be computed by applying central difference operators δ_{x^α} to the discrete scale-space representation obtained by convolution with the discrete analogue of the Gaussian kernel (66). This operation then leads to equivalent discrete derivative approximation kernels of the form

$$T_{\text{disc},x^\alpha}(n; s) = (\delta_{x^\alpha} T_{\text{disc}})(n; s), \quad (71)$$

although with the important distinction that such equivalent discrete approximation kernels should never be used for practical numerical computations, but instead just be considered as a conceptual modelling tool, for representing the mathematically equivalent effect of the discrete derivative approximation method.

The reason for this is that in situations, when multiple Gaussian derivative responses are to be computed from the same input signal f for different orders of differentiation α , it is computationally much more efficient to instead just perform the spatial smoothing operation with the discrete analogue of the Gaussian kernel once and for all, and then apply the small-support central difference operators δ_{x^α} for the different orders of differentiation. In this way, a substantial amount of computation can be saved in situations when several Gaussian derivative responses are to be computed for different orders of differentiation. This implementation approach thereby has substantial computational advantages, when using discrete approximations of Gaussian derivative responses as the basic computational primitives for defining the layers in deep networks.

Other conceptual advantages of this discretisation method for Gaussian derivative computation are also that the resulting discrete derivative approximations obey a cascade smoothing property over scales

$$L_{\text{disc}}(\cdot; s_2) = T_{\text{disc}}(\cdot; s_2 - s_1) * L_{\text{disc}}(\cdot; s_1) \quad (72)$$

between any pair of scale levels $s_2 > s_1$, and which then also implies that the scale-space properties of the zero-order discrete analogue of the Gaussian kernel, in terms of *e.g.*, non-creation of new local extrema or new zero-crossings from finer to coarser levels of scale, are

also carried over to the resulting discrete approximations of Gaussian derivative responses. In these respects, this discretisation approach, of combining the discrete analogue of the Gaussian kernel with central differences, has specific both theoretical and computational advantages at very fine scale levels.

B.10 Hybrid discretisation based on the normalised sampled Gaussian kernel in combination with central differences

Inspired by the computational efficiency of the discrete derivative approximations described in the previous section, and obtained by convolution with the discrete analogue of the Gaussian kernel according to (66) followed by central differences δ_{x^α} , we will in this paper analyse the effects of computing corresponding discrete derivative approximations, by applying central difference operators δ_{x^α} to the result of smoothing a discrete signal with the normalised sampled Gaussian kernel according to (63).

The motivation for this operation is again to obtain substantially higher computational efficiency compared to explicit convolutions with multiple sampled Gaussian derivative kernels according to (69), when to compute Gaussian derivative responses for multiple orders of differentiation α .

The equivalent convolution kernels for this discretisation method will then be of the form

$$T_{\text{hybr-sampl},x^\alpha}(n; s) = (\delta_{x^\alpha} T_{\text{normsampl}})(n; s). \quad (73)$$

As for the above discretisation method with convolution with the discrete analogue of the Gaussian kernel followed by central differences, the intention with this definition of a corresponding discrete equivalent convolution kernel is, however, again only to be used a theoretical modelling tool, and not for any actual implementations. The reason for this is that, in situations when multiple Gaussian derivative responses are to be computed for the same input signal f , it is computationally much more efficient to first perform the smoothing with the normalised sampled Gaussian kernel once and for all, and then apply each central difference operator δ_{x^α} .

This hybrid discretisation method was proposed among suggestions to future work in Section 6 in (Lindeberg 2024) and with theoretical properties of that discretisation method analysed in Footnote 13 in that paper. The quantitative performance of this hybrid discretisation method was, however, not evaluated experimentally, which is a main subject of this paper.

B.11 Hybrid discretisation based on the integrated Gaussian kernel in combination with central differences

In analogy with the treatment above concerning the discretisation method, based on discrete convolution with the normalised sampled Gaussian kernel (63) followed by central differences δ_{x^α} , we can also in a corresponding manner instead use the integrated Gaussian kernel (64) as an initial smoothing step and then apply central differences δ_{x^α} to the smoothed data, corresponding to the following equivalent discrete derivative approximation kernel

$$T_{\text{hybr-int},x^\alpha}(n; s) = (\delta_{x^\alpha} T_{\text{int}})(n; s). \quad (74)$$

Again, this equivalent convolution kernel is, however, not intended to be used for practical implementations, since in situations when Gaussian derivative responses are to be computed for different orders of differentiation α for the same input signal, it is computationally much more efficient to just perform the spatial smoothing operation once and

for all and then apply the different central difference operators $\delta_{x\alpha}$ to the smoothed signal. In this way, when Gaussian derivative responses are to be computed from the same signal f for different orders of differentiation α , it will be computationally much more efficient to perform the computations in this way, compared to *e.g.* performing explicit convolutions with a corresponding set of integrated Gaussian derivative kernels according to (9).

This hybrid discretisation method was also proposed among suggestions to future work in Section 6 in (Lindeberg 2024) and with theoretical properties of that discretisation method analysed in Footnote 13 in that paper. The quantitative performance of this hybrid discretisation method was, however, not evaluated experimentally, which is a main subject of this paper.

C Definition of discrete model signals for quantitatively evaluating the performance of the different discrete approximations of Gaussian derivative operator

This appendix section describes how the discrete input model signals (Gaussian blobs for interest point detection, diffuse edges for edge detection, or Gaussian ridges for ridge detection) are generated for evaluating the scale selection properties for the different types of feature detectors (Laplacian interest point detection, determinant of the Hessian interest point detection, gradient magnitude edge detection or principal curvature ridge detection) experimentally evaluated in Section 3.2. Specifically, this appendix section describes how the methods for discrete approximations of the continuous input signals are determined for the different methods for discrete approximations of the Gaussian derivative operators.

C.1 Methodology for defining the discrete input data for the scale selection experiments

When generating input data for different values of the reference scale σ_0 , we

- for the purpose of Laplacian or determinant of the Hessian interest point detection, for generating a discrete blob, to be used as input for computing the scale-normalised differential entities $(\nabla_{\text{norm}}^2 L)(x, y; s)$ and $(\det \mathcal{H}_{\text{norm}} L)(x, y; s)$ for interest point detection at multiple scales, we use a discrete approximation of Gaussian blob (Equation (25)), obtained by convolving a 2-D discrete delta function

$$\delta(x, y) = \begin{cases} 1 & \text{if } (x, y) = (0, 0), \\ 0 & \text{otherwise,} \end{cases} \quad (75)$$

with a discrete approximation of a Gaussian kernel along each dimension,

- for the purpose of edge detection, for generating a discrete diffuse edge, to be used as input for computing the scale-normalised gradient magnitude $L_{v,\text{norm}}(0, 0; s)$ at multiple scales, we use a discrete approximation of a diffuse edge (Equation (30)), obtained by convolving an ideal step edge function

$$H(x) = \begin{cases} +1/2 & \text{if } x > 0, \\ 0 & \text{if } x = 0, \\ -1/2 & \text{if } x < 0, \end{cases} \quad (76)$$

with a discrete approximation of a Gaussian kernel along the x -direction,

- for the purpose of ridge detection, for generating a discrete Gaussian ridge, to be used as input for computing the scale-normalised principal curvature measure $L_{pp,\text{norm}}(0, 0; s)$ at multiple scales, we use a discrete approximation of a Gaussian ridge (34), obtained by convolving the 2-D extension of a 1-D discrete delta function

$$\delta(x) = \begin{cases} 1 & \text{if } x = 0, \\ 0 & \text{otherwise,} \end{cases} \quad (77)$$

along the y -direction with a discrete approximation of a Gaussian kernel along the x -direction.

Since a main purpose of the experiments defined in Section 2.2 and reported in Section 3.2 is to measure the *consistency* between the characteristic scales in the input with the characteristic scale values obtained by multi-scale processing of the input data, we choose the discretisation method for generating the input data for the scale estimation algorithm in relation to the discretisation method used for defining the discrete derivative approximations in the following way:

- when evaluating the discretisation based on the discrete analogue of Gaussian derivatives, we use the discrete analogue of the Gaussian kernel as the discrete convolution kernel when generating the input data,
- when evaluating the discretisation method based on sampled Gaussian derivatives, we use the sampled Gaussian kernel as the discrete convolution kernel when generating the input data,
- when evaluating the discretisation method based on integrated Gaussian derivatives, we use the integrated Gaussian kernel as the discrete convolution kernel when generating the input data,
- when evaluating the hybrid method, based on convolution with the normalised sampled Gaussian kernel followed by central differences, we use the normalised sampled Gaussian kernel as the discrete convolution kernel when generating the input data, and
- when evaluating the hybrid method, based on convolution with the integrated Gaussian kernel followed by central differences, we use the integrated Gaussian kernel as the discrete convolution kernel when generating the input data.

Thus, since the purpose of the experiments in Section 3.2 in the main text is to measure the mutual consistency between the discrete approximations of Gaussian derivative responses between different scales, the intention is to use an as conceptually similar discretisation method for generating the input data, as will be used when analysing the same data by the feature detection algorithms. Since the generation of the input data will, however, hence differ between the different discretisation methods for Gaussian derivatives, some care therefore needs to be taken when interpreting the experimental results.

C.2 Motivation for the experimental paradigm in terms of internal consistency of scale estimates

The motivation for evaluating the performance of the different use cases for feature detection with automatic scale selection with regard to the internal consistency between the discrete approximations of the input and the discrete approximations of the Gaussian derivative kernels, as opposed to comparing all the different discretisation methods relative to the same ground truth, is that the definition of a common ground truth itself becomes very problematic at very fine scale levels, in turn, because of the quantitative measurement of the amount of effective discrete blur for a given value of the scale parameter s may differ significantly between the different discrete approximation methods at very fine scales, although the value of the underlying scale parameter is the same (see Sections 2.8.2–2.8.4 and 3.8.2 in Lindeberg (2024) as well as Figures 2 and 3 in this paper for numerical quantifications of this property).

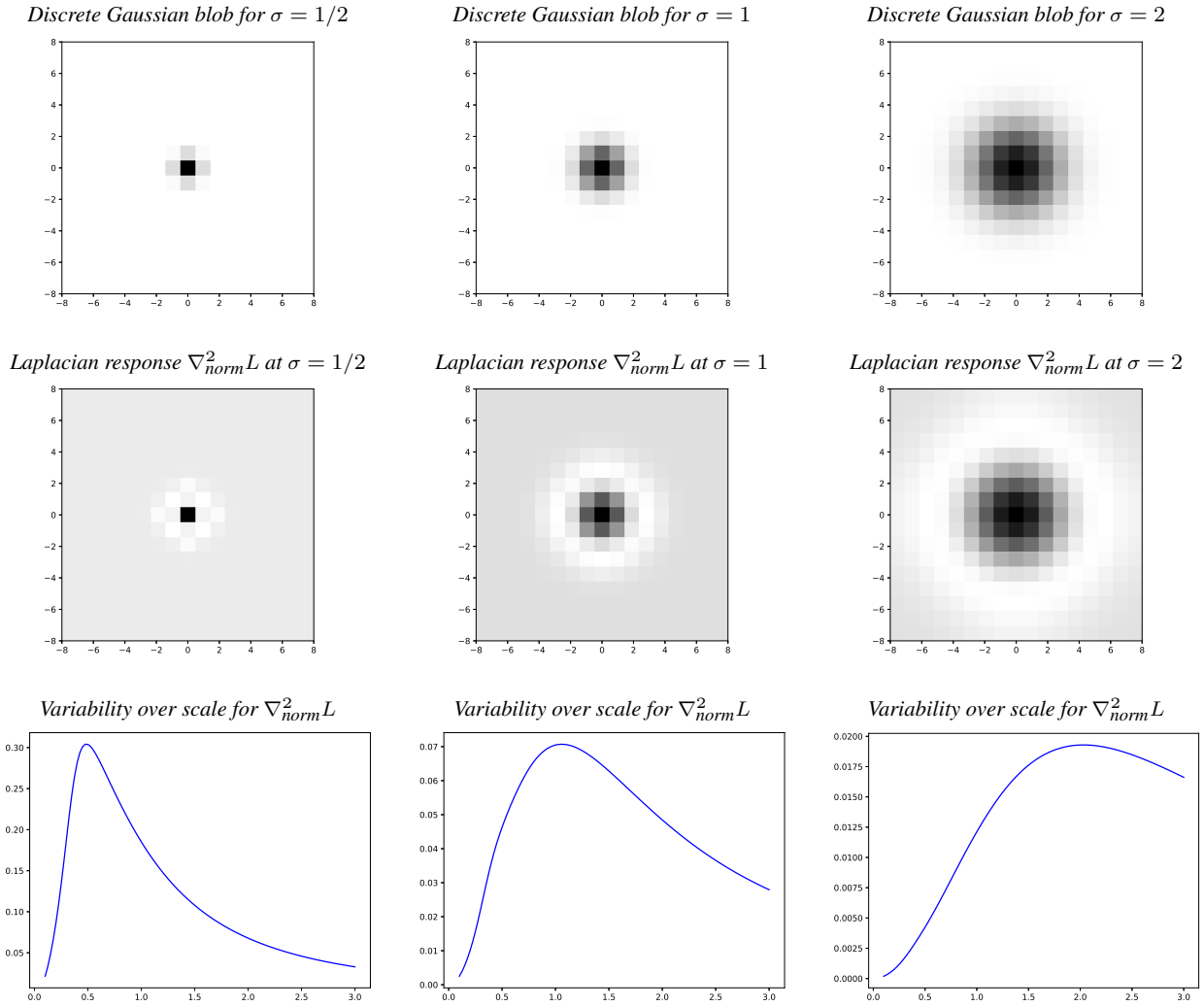


Fig. 6: Visualisation of the conceptual steps involved when computing scale estimates using *Laplacian interest point detection with automatic scale selection*, here using the hybrid discretisation method based on convolution with normalised sampled Gaussian kernels followed by central differences. **(top row)** Input images for three different sizes $\sigma_0 = 1/2$, $\sigma_0 = 1$ and $\sigma_0 = 2$ of the discrete Gaussian blobs (with the contrast reversed in the visualisation). **(middle row)** The result of computing a discrete approximation of the Laplacian response $\nabla L = L_{xx} + L_{yy}$ for the different input images in the top row, at the scale levels $\sigma = 1/2$, $\sigma = 1$ and $\sigma = 2$, respectively. **(bottom row)** Graphs of the variability over scale σ for (the negative value of) the scale-normalised Laplacian response $\nabla_{\text{norm}}^2 L = \sigma^2 (L_{xx} + L_{yy})$ for each one of the images in the top row. Note that the selected scales $\hat{\sigma}$, where the maxima in these graphs are assumed, do rather well correspond to the scales σ_0 in the input data.

D Visualisations of image feature models, differential feature responses and variabilities in scale-normalised derivative responses over scale, which underlie the computation of scale estimates for different inherent scale values s_0 in the input data

Figures 6–9 provide visualisations of the conceptual steps involved, when defining the scale estimates in Section 2.2, that are then quantitatively evaluated in Section 3.2.

In these figures, we specifically show:

- *discretisations of the idealised model signals*, that are used as input:
 - Gaussian blobs, according to Equation (25), for Laplacian and determinant of the Hessian interest point detection,

- diffuse edges, according to Equation (30), for gradient magnitude based edge detection, and
 - Gaussian ridges, according to Equation (34), for principal curvature based ridge detection,
- for different choices of the scale values $\sigma_0 \in \{\frac{1}{2}, 1, 2\}$,
- *discrete approximations of the differential feature strength measures* at the scales $\hat{\sigma} = \sigma_0$, where the corresponding fully continuous differential feature strength measures $\mathcal{D}_{\text{norm}} L$ would assume their local extrema over scale σ at the image center for each type of feature detector:
 - the scale-normalised Laplacian operator $\nabla_{\text{norm}}^2 L$, according to Equation (23),
 - the scale-normalised determinant of the Hessian $\det \mathcal{H}_{\text{norm}} L$, according to Equation (24),
 - the scale-normalised gradient magnitude $L_{v,\text{norm}}$, according to Equation (28), and

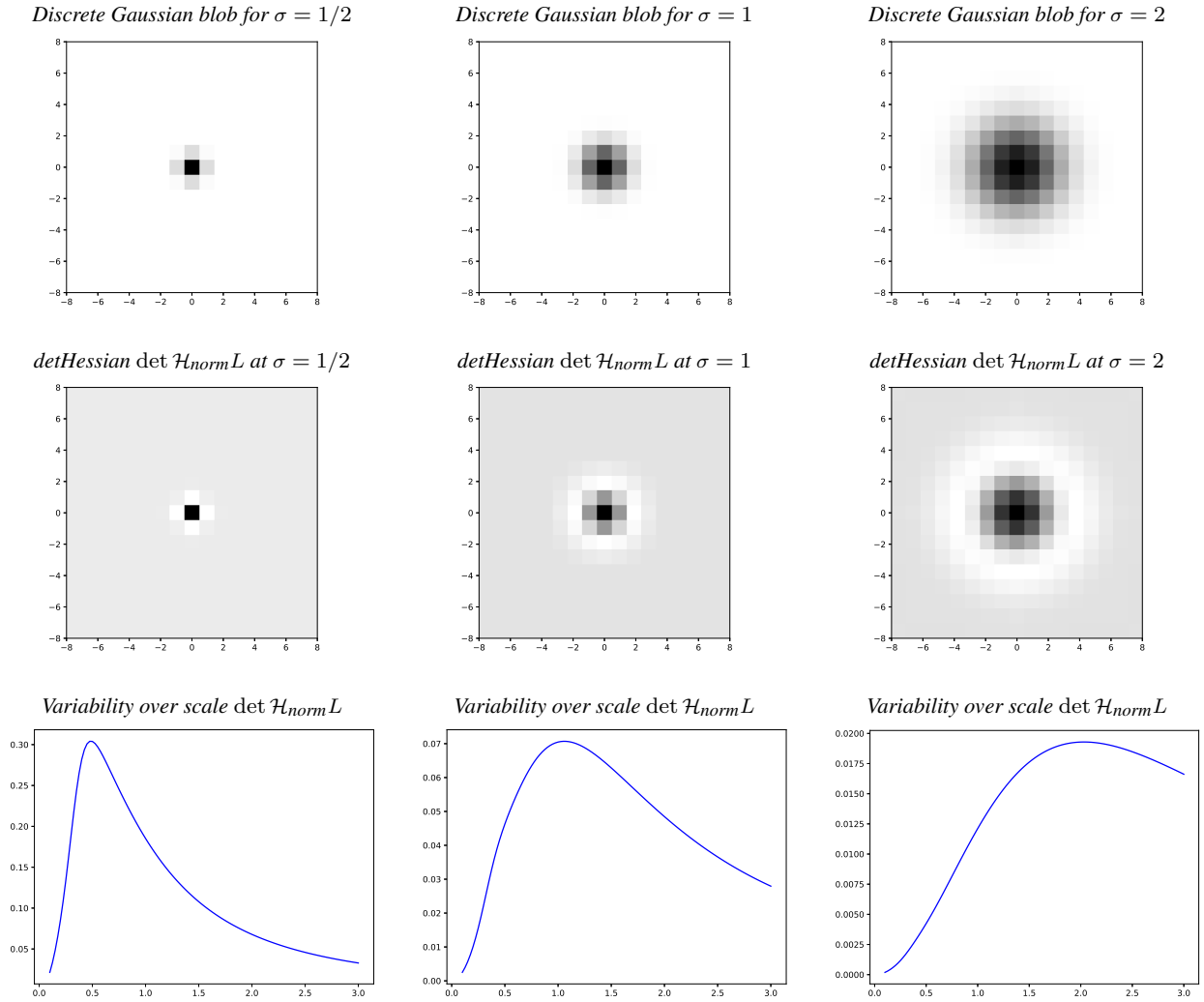


Fig. 7: Visualisation of the conceptual steps involved when computing scale estimates using *determinant of the Hessian interest point detection with automatic scale selection*, here using the hybrid discretisation method based on convolution with normalised sampled Gaussian kernels followed by central differences. **(top row)** Input images for three different sizes $\sigma_0 = 1/2$, $\sigma_0 = 1$ and $\sigma_0 = 2$ of the discrete Gaussian blobs (with the contrast reversed in the visualisation). **(middle row)** The result of computing a discrete approximation of the determinant of the Hessian response $\det \mathcal{H}L = L_{xx} L_{yy} - L_{xy}^2$ for the different input images in the top row, at the scale levels $\sigma = 1/2$, $\sigma = 1$ and $\sigma = 2$, respectively (again with the contrast reversed in the visualisation). **(bottom row)** Graphs of the variability over scale σ for (the negative value of) the scale-normalised determinant of the Hessian response $\det \mathcal{H}_{\text{norm}}L = \sigma^4 (L_{xx} L_{yy} - L_{xy}^2)$ for each one of the images in the top row. Note that the selected scales $\hat{\sigma}$, where the maxima in these graphs are assumed, do rather well correspond to the scales σ_0 in the input data.

- the scale-normalized principal curvature based ridge strength measure $L_{pp,\text{norm}}$, according to Equation (32), for the different choices of the scale values $\sigma_0 \in \{\frac{1}{2}, 1, 2\}$ for the input data, as well as
- *graphs of the variability over scale σ for discrete approximations of these scale-normalised measures of feature strength*, demonstrating that the selected scale values, obtained from the local extrema over scales, do reasonably well reflect the inherent characteristic scales σ_0 in the input data for the resulting scale selection methods.

For the visualisations in this appendix, we have in all these figures used:

- the hybrid discretisation method, based on smoothing with the normalised sampled Gaussian kernel followed by central differences, according to Appendix B.10.

In the actual quantitative performance evaluation experiments reported in Section 2.2, corresponding computations are additionally performed for the four other discrete derivative approximation methods based on:

- the sampled Gaussian derivative kernels, according to Appendix B.7,
- the integrated Gaussian derivative kernels, according to Appendix B.8,
- the discrete analogue of the Gaussian kernel combined with central difference operators, according to Appendix B.9, and
- smoothing with the integrated Gaussian kernel followed by central difference operators, according to Appendix B.11.

The graphs in Figures 4 and 5 do additionally show the results of numerical scale estimates for a much denser set of scale values $\sigma_0 \in \{\frac{1}{3}, 2\}$.

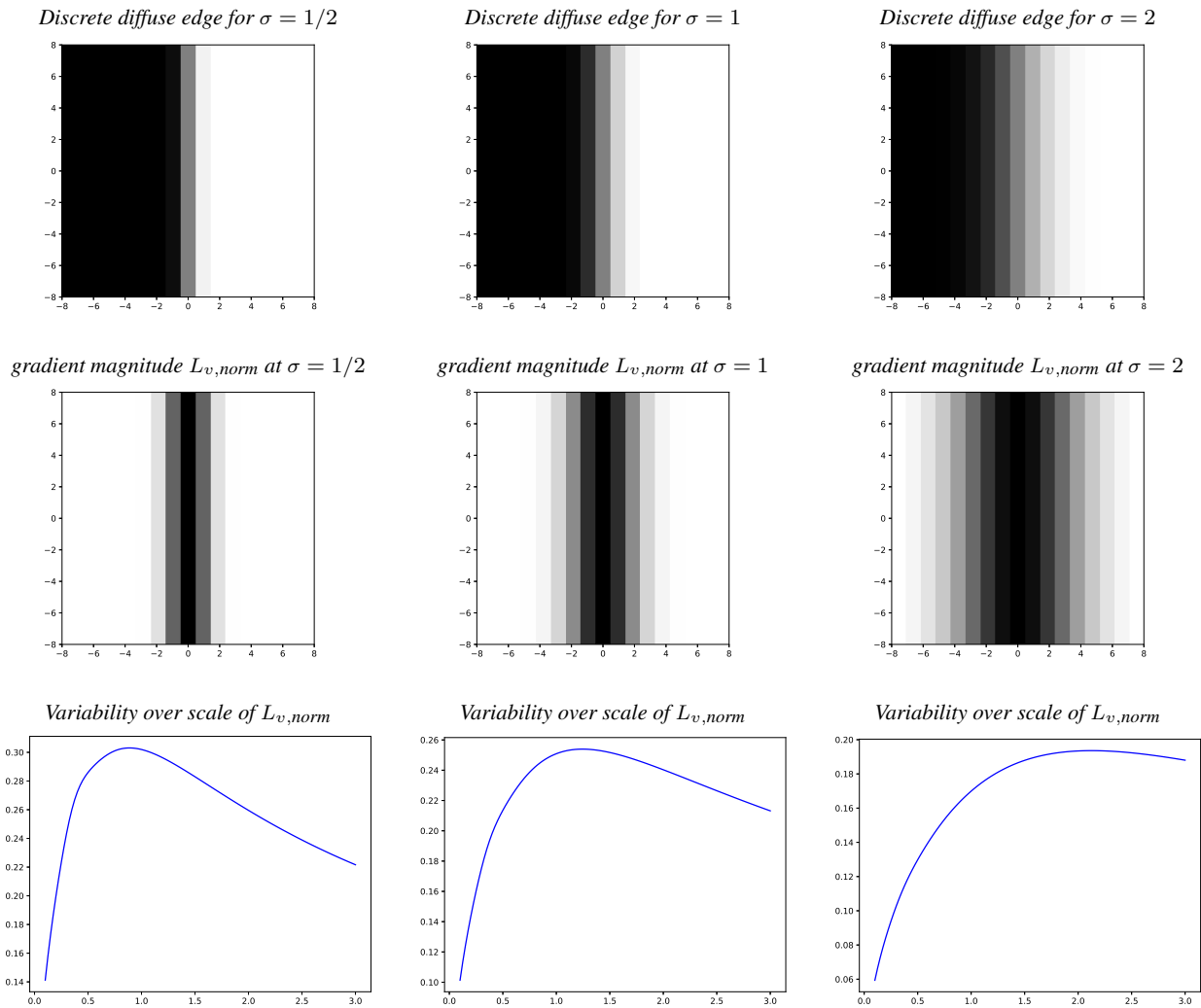


Fig. 8: Visualisation of the conceptual steps involved when computing scale estimates using *gradient magnitude based edge detection with automatic scale selection*, here using the hybrid discretisation method based on convolution with normalised sampled Gaussian kernels followed by central differences. **(top row)** Input images for three degrees of diffuseness $\sigma_0 = 1/2$, $\sigma_0 = 1$ and $\sigma_0 = 2$ for the discrete diffuse edges. **(middle row)** The result of computing a discrete approximation of the gradient magnitude $L_v = \sqrt{L_x^2 + L_y^2}$ for the different input images in the top row, at the scale levels $\sigma = 1/2$, $\sigma = 1$ and $\sigma = 2$, respectively (with the contrast reversed in the visualisation). **(bottom row)** Graphs of the variability over scale σ for the scale-normalised gradient magnitude $L_{v,norm} = \sigma^\gamma \sqrt{L_x^2 + L_y^2}$ for each one of the images in the top row, using the scale normalisation power $\gamma = 1/2$. Note that the selected scales $\hat{\sigma}$, where the maxima in these graphs are assumed, do rather well correspond to the scales σ_0 in the input data.

References

- M. Abramowitz and I. A. Stegun, editors. *Handbook of Mathematical Functions*. Applied Mathematics Series. National Bureau of Standards, US Government Printing Office, 55 edition, 1964. (Reprinted by Dover Publications).
- K. Åström and A. Heyden. Stochastic analysis of image acquisition and scale-space smoothing. In J. Sporring, M. Nielsen, L. Florack, and P. Johansen, editors, *Gaussian Scale-Space Theory: Proc. PhD School on Scale-Space Theory*, pages 129–136. Springer, 1997.
- H. Bay, A. Ess, T. Tuytelaars, and L. van Gool. Speeded up robust features (SURF). *Computer Vision and Image Understanding*, 110(3):346–359, 2008.
- E. J. Bekkers. B-spline CNNs on Lie groups. *International Conference on Learning Representations (ICLR 2020)*, 2020. <https://openreview.net/forum?id=H1gBhkBFDH>, preprint at arXiv:1909.12057.
- H. Bouma, A. Vilanova, J. O. Bescós, B. ter Haar Romeny, and F. A. Gerritsen. Fast and accurate Gaussian derivatives based on B-splines. In F. Gallari, A. Murli, and N. Paragios, editors, *Proc. Scale Space and Variational Methods in Computer Vision (SSVM 2007)*, volume 4485 of *Springer LNCS*, pages 406–417, May. 2007.
- L. Bretzner and T. Lindeberg. Feature tracking with automatic selection of spatial scales. *Computer Vision and Image Understanding*, 71(3):385–392, Sep. 1998.
- P. J. Burt and E. H. Adelson. The Laplacian pyramid as a compact image code. *IEEE Trans. Communications*, 9(4):532–540, 1983.
- D. Charalampidis. Recursive implementation of the Gaussian filter using truncated cosine functions. *IEEE Transactions on Signal Processing*, 64(14):3554–3565, 2016.

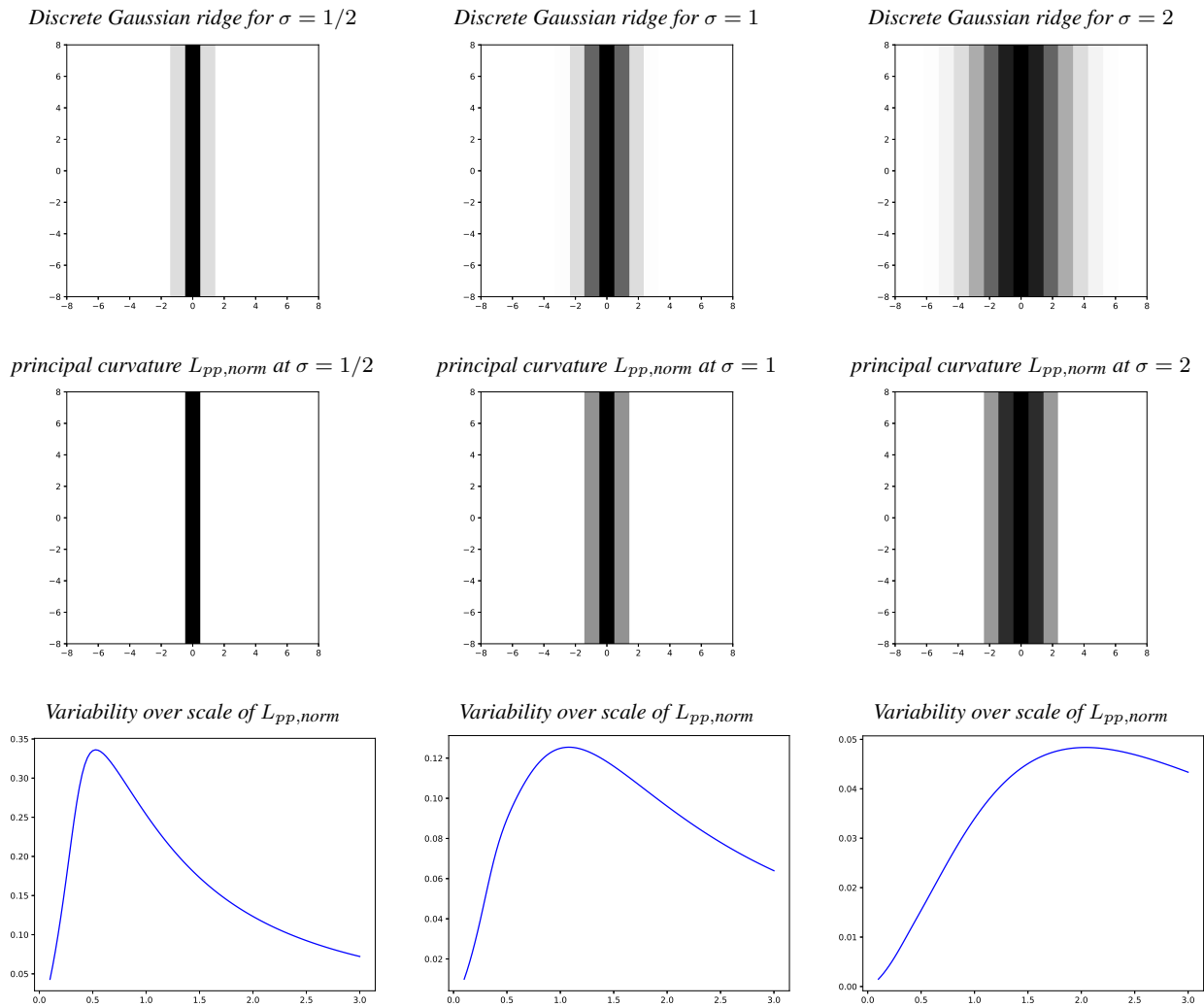


Fig. 9: Visualisation of the conceptual steps involved when computing scale estimates using *principal curvature based ridge detection with automatic scale selection*, here using the hybrid discretisation method based on convolution with normalised sampled Gaussian kernels followed by central differences. **(top row)** Input images for three different widths $\sigma_0 = 1/2$, $\sigma_0 = 1$ and $\sigma_0 = 2$ for the discrete Gaussian ridges. **(middle row)** The result of computing a discrete approximation of the principal curvature based ridge strength measure $L_{pp} = L_{xx} + L_{yy} - \sqrt{(L_{xx} - L_{yy})^2 + 4L_{xy}^2}$ for the different input images in the top row, at the scale levels $\sigma = 1/2$, $\sigma = 1$ and $\sigma = 2$, respectively (with the contrast reversed in the visualisation). **(bottom row)** Graphs of the variability over scale σ for the scale-normalised principal curvature based ridge strength measure $L_{pp,norm} = \sigma^{2\gamma} (L_{xx} + L_{yy} - \sqrt{(L_{xx} - L_{yy})^2 + 4L_{xy}^2})$ for each one of the images in the top row, using the scale normalisation power $\gamma = 3/4$. Note that the selected scales $\hat{\sigma}$, where the maxima in these graphs are assumed, do rather well correspond to the scales σ_0 in the input data.

O. Chomat, V. de Verdiere, D. Hall, and J. Crowley. Local scale selection for Gaussian based description techniques. In *Proc. European Conf. on Computer Vision (ECCV 2000)*, volume 1842 of *Springer LNCS*, pages I:117–133, Dublin, Ireland, 2000.

J. L. Crowley and O. Riff. Fast computation of scale normalised Gaussian receptive fields. In L. Griffin and M. Lillholm, editors, *Proc. Scale-Space Methods in Computer Vision (Scale-Space'03)*, volume 2695 of *Springer LNCS*, pages 584–598, 2003.

J. L. Crowley and R. M. Stern. Fast computation of the difference of low pass transform. *IEEE Transactions on Pattern Analysis and Machine Intelligence*, 6(2):212–222, 1984.

I. Daubechies. *Ten Lectures on Wavelets*. SIAM, Philadelphia, 1992.

L. Debnath and F. A. Shah. *Wavelet Transforms and Their Applications*. Springer, 2002.

R. Deriche. Recursively implementing the Gaussian and its derivatives. In *Proc. International Conference on Image Processing (ICIP'92)*, pages 263–267, 1992.

G. Farnebäck and C.-F. Westin. Improving Deriche-style recursive Gaussian filters. *Journal of Mathematical Imaging and Vision*, 26(3):293–299, 2006.

L. M. J. Florack. *Image Structure*. Series in Mathematical Imaging and Vision. Springer, 1997.

H. Gavilima-Pilataxi and J. Ibarra-Fiallo. Multi-channel Gaussian derivative neural networks for crowd analysis. In *Proc. International Conference on Pattern Recognition Systems (ICPRS 2023)*,

- pages 1–7, 2023.
- J.-M. Geusebroek, A. W. M. Smeulders, and J. van de Weijer. Fast anisotropic Gauss filtering. *IEEE Transactions on Image Processing*, 12(8):938–943, 2003.
- T. Iijima. Basic theory on normalization of pattern (in case of typical one-dimensional pattern). *Bulletin of the Electrotechnical Laboratory*, 26:368–388, 1962. (in Japanese).
- J.-J. Jacobsen, J. van Gemert, Z. Lou, and A. W. M. Smeulders. Structured receptive fields in CNNs. In *Proc. Computer Vision and Pattern Recognition (CVPR 2016)*, pages 2610–2619, 2016.
- J. J. Koenderink. The structure of images. *Biological Cybernetics*, 50(5):363–370, 1984.
- J. J. Koenderink and A. J. van Doorn. Representation of local geometry in the visual system. *Biological Cybernetics*, 55(6):367–375, 1987.
- J. J. Koenderink and A. J. van Doorn. Generic neighborhood operators. *IEEE Transactions on Pattern Analysis and Machine Intelligence*, 14(6):597–605, Jun. 1992.
- J.-Y. Lim and H. S. Stiehl. A generalized discrete scale-space formulation for 2-D and 3-D signals. In L. Griffin and M. Lillholm, editors, *Proc. Scale-Space Methods in Computer Vision (Scale-Space'03)*, volume 2695 of *Springer LNCS*, pages 132–147. Springer, Jun. 2003.
- T. Lindeberg. Scale-space for discrete signals. *IEEE Transactions on Pattern Analysis and Machine Intelligence*, 12(3):234–254, Mar. 1990.
- T. Lindeberg. *Scale-Space Theory in Computer Vision*. Springer, 1993a.
- T. Lindeberg. Discrete derivative approximations with scale-space properties: A basis for low-level feature extraction. *Journal of Mathematical Imaging and Vision*, 3(4):349–376, Nov. 1993b.
- T. Lindeberg. Scale-space theory: A basic tool for analysing structures at different scales. *Journal of Applied Statistics*, 21(2):225–270, 1994. Also available from <http://www.csc.kth.se/~tony/abstracts/Lin94-SI-abstract.html>.
- T. Lindeberg. On the axiomatic foundations of linear scale-space. In J. Sporring, M. Nielsen, L. Florack, and P. Johansen, editors, *Gaussian Scale-Space Theory: Proc. PhD School on Scale-Space Theory*, pages 75–97. Copenhagen, Denmark, May. 1996. Springer.
- T. Lindeberg. Feature detection with automatic scale selection. *International Journal of Computer Vision*, 30(2):77–116, 1998a.
- T. Lindeberg. Edge detection and ridge detection with automatic scale selection. *International Journal of Computer Vision*, 30(2):117–154, 1998b.
- T. Lindeberg. Principles for automatic scale selection. In *Handbook on Computer Vision and Applications*, pages 239–274. Academic Press, Boston, USA, 1999. Also available from <http://www.csc.kth.se/cvapp/abstracts/cvap222.html>.
- T. Lindeberg. Scale-space. In B. Wah, editor, *Encyclopedia of Computer Science and Engineering*, pages 2495–2504. John Wiley and Sons, Hoboken, New Jersey, 2008.
- T. Lindeberg. Generalized Gaussian scale-space axiomatics comprising linear scale-space, affine scale-space and spatio-temporal scale-space. *Journal of Mathematical Imaging and Vision*, 40(1):36–81, 2011.
- T. Lindeberg. Scale selection properties of generalized scale-space interest point detectors. *Journal of Mathematical Imaging and Vision*, 46(2):177–210, 2013a.
- T. Lindeberg. Generalized axiomatic scale-space theory. In P. Hawkes, editor, *Advances in Imaging and Electron Physics*, volume 178, pages 1–96. Elsevier, 2013b.
- T. Lindeberg. Image matching using generalized scale-space interest points. *Journal of Mathematical Imaging and Vision*, 52(1):3–36, 2015.
- T. Lindeberg. Dense scale selection over space, time and space-time. *SIAM Journal on Imaging Sciences*, 11(1):407–441, 2018.
- T. Lindeberg. Provably scale-covariant continuous hierarchical networks based on scale-normalized differential expressions coupled in cascade. *Journal of Mathematical Imaging and Vision*, 62(1):120–148, 2020.
- T. Lindeberg. Scale selection. In K. Ikeuchi, editor, *Computer Vision*, pages 1110–1123. Springer, 2021a. https://doi.org/10.1007/978-3-030-03243-2_242-1.
- T. Lindeberg. Normative theory of visual receptive fields. *Heliyon*, 7(1):e05897:1–20, 2021b. doi: 10.1016/j.heliyon.2021.e05897.
- T. Lindeberg. Scale-covariant and scale-invariant Gaussian derivative networks. In A. Elmoataz, J. Fadili, Y. QuÃ©au, J. Rabin, and L. Simon, editors, *Proc. Scale Space and Variational Methods in Computer Vision (SSVM 2021)*, volume 12679 of *Springer LNCS*, pages 3–14, 2021c.
- T. Lindeberg. Scale-covariant and scale-invariant Gaussian derivative networks. *Journal of Mathematical Imaging and Vision*, 64(3):223–242, 2022.
- T. Lindeberg. Discrete approximations of Gaussian smoothing and Gaussian derivatives. *Journal of Mathematical Imaging and Vision*, 66(5):759–800, 2024.
- T. Lindeberg and L. Bretzner. Real-time scale selection in hybrid multi-scale representations. In L. Griffin and M. Lillholm, editors, *Proc. Scale-Space Methods in Computer Vision (Scale-Space'03)*, volume 2695 of *Springer LNCS*, pages 148–163. Springer, 2003.
- D. G. Lowe. Distinctive image features from scale-invariant keypoints. *International Journal of Computer Vision*, 60(2):91–110, 2004.
- S. Mallat. Multifrequency channel decompositions of images and wavelet models. *IEEE Trans. Acoustics, Speech and Signal Processing*, 37:2091–2110, 1989a.
- S. Mallat. Understanding deep convolutional networks. *Phil. Trans. Royal Society A*, 374(2065):20150203, 2016.
- S. G. Mallat. A theory for multiresolution signal decomposition: The wavelet representation. *IEEE Transactions on Pattern Analysis and Machine Intelligence*, 11(7):674–694, 1989b.
- S. G. Mallat. *A Wavelet Tour of Signal Processing*. Academic Press, 1999.
- Y. Meyer. *Wavelets and Operators: Volume 1*. Cambridge University Press, 1992.
- V. Penaud-Polge, S. Velasco-Forero, and J. Angulo. Fully trainable Gaussian derivative convolutional layer. In *International Conference on Image Processing (ICIP 2022)*, pages 2421–2425, 2022.
- S. L. Pinteá, N. Tömen, S. F. Goes, M. Loog, and J. C. van Gemert. Resolution learning in deep convolutional networks using scale-space theory. *IEEE Trans. Image Processing*, 30:8342–8353, 2021.
- I. Rey-Otero and M. Delbracio. Computing an exact Gaussian scale-space. *Image Processing On Line*, 6:8–26, 2016.
- M. Sangalli, S. Blusseau, S. Velasco-Forero, and J. Angulo. Scale equivariant U-net. In *Proc. British Machine Vision Conference (BMVC 2022)*, page 763, 2022.
- E. P. Simoncelli and W. T. Freeman. The steerable pyramid: A flexible architecture for multi-scale derivative computation. In *Proc. International Conference on Image Processing (ICIP'95)*, volume 3, pages 444–447, Washington DC, 1995.
- E. P. Simoncelli, W. T. Freeman, E. H. Adelson, and D. J. Heeger. Shiftable multi-scale transforms. *IEEE Trans. Information Theory*, 38(2):587–607, 1992.
- A. Slavík and P. Stehlík. Dynamic diffusion-type equations on discrete-space domains. *Journal of Mathematical Analysis and Applications*, 427(1):525–545, 2015.
- J. Sporring, M. Nielsen, L. Florack, and P. Johansen, editors. *Gaussian Scale-Space Theory: Proc. PhD School on Scale-Space Theory*. Series in Mathematical Imaging and Vision. Springer, Copenhagen, Denmark, 1997.
- A. Teolis. *Computational Signal Processing with Wavelets*. Birkhäuser, 1998.

- B. ter Haar Romeny. *Front-End Vision and Multi-Scale Image Analysis*. Springer, 2003.
- M. Tschirsich and A. Kuijper. Notes on discrete Gaussian scale space. *Journal of Mathematical Imaging and Vision*, 51:106–123, 2015.
- M. Unser, A. Aldroubi, and M. Eden. Fast B-spline transforms for continuous image representation and interpolation. *IEEE Transactions on Pattern Analysis and Machine Intelligence*, 13(3):277–285, 1991.
- M. Unser, A. Aldroubi, and M. Eden. B-spline signal processing. I. Theory. *IEEE Transactions on Signal Processing*, 41(2):821–833, 1993.
- L. J. van Vliet, I. T. Young, and P. W. Verbeek. Recursive Gaussian derivative filters. In *International Conference on Pattern Recognition*, volume 1, pages 509–514, 1998.
- Y.-P. Wang. Image representations using multiscale differential operators. *IEEE Transactions on Image Processing*, 8(12):1757–1771, 1999.
- Y.-P. Wang and S. L. Lee. Scale-space derived from B-splines. *IEEE Transactions on Pattern Analysis and Machine Intelligence*, 20(10):1040–1055, 1998.
- J. Weickert, S. Ishikawa, and A. Imiya. Linear scale-space has first been proposed in Japan. *Journal of Mathematical Imaging and Vision*, 10(3):237–252, 1999.
- A. P. Witkin. Scale-space filtering. In *Proc. 8th Int. Joint Conf. Art. Intell.*, pages 1019–1022, Karlsruhe, Germany, Aug. 1983.
- D. Worrall and M. Welling. Deep scale-spaces: Equivariance over scale. In *Advances in Neural Information Processing Systems (NeurIPS 2019)*, pages 7366–7378, 2019.
- Y. Yang, S. Dasmahapatra, and S. Mahmoodi. Scale-equivariant UNet for histopathology image segmentation. *arXiv preprint arXiv:2304.04595*, 2023.
- I. T. Young and L. J. van Vliet. Recursive implementation of the Gaussian filter. *Signal Processing*, 44(2):139–151, 1995.
- Q. Zheng, M. Gong, X. You, and D. Tao. A unified B-spline framework for scale-invariant keypoint detection. *International Journal of Computer Vision*, 130(3):777–799, 2022.